Mechanism of Cholesterol-Mediated Retinal Pigment Epithelium Dysfunction as a Model for Dry Age-Related Macular Degeneration

Mechanism of Cholesterol-Mediated Retinal Pigment Epithelium Dysfunction as a Model for Dry Age-Related Macular Degeneration

by

Eun Young (Alice) Choi

Harvard-M.I.T. Division of Health Sciences and Technology

Submitted in Partial Fulfillment of the Requirements for the M.D. Degree with Honors in a Special Field at Harvard Medical School

February 4, 2019

Area of Concentration: Molecular Biology

Project Advisor: Patricia A. D'Amore, Ph.D., M.B.A.

Author's Prior Degrees: B.S. in Chemistry

I have reviewed this thesis. It represents work done by the author under my supervision and guidance.

Patricia A. D'Amore, PhD

Digitally signed by Patricia A. D'Amore, PhD
DN: cn=Patricia A. D'Amore, PhD, o=Schepens Eye Rearch Institute-Mass. Eye & Ear, ou, email=patricia_damore@meei.harvard.edu, c=US
Date: 2019.02.03 14:42:34 -05'00'

Faculty Supervisor's Signature

Thesis Statement

The work presented here represents that of my own, except where indicated and appropriate credit is given.

Table of Contents

Abstract

Purpose: There is currently no established treatment for dry age-related macular degeneration (AMD), which is characterized by a progressive degeneration and death of the retinal pigment epithelium (RPE). While the etiology of AMD is not completely understood, lipid accumulation and inflammation are strongly associated with disease progression. Studies suggest that lipoproteins which accumulate in sub-retinal space and become oxidized are a major contributor to RPE dysfunction and death. Peroxisome proliferator-activated receptors (PPARs) are a family of lipid-activated transcription factors that are involved in lipid metabolism and inflammatory processes. We examined a variety of PPARγ agonists and found that troglitazone is uniquely effective in protecting the RPE against oxLDL-induced cell death. The purpose of this study is to elucidate the mechanism of troglitazone in its protection of RPE against oxLDL-induced cell death.

Methods: SiRNA was used to knock down PPARγ in ARPE-19 cells, and the expression of PPARγ was determined by RT-PCR. After treatment with oxLDL ± troglitazone, rosiglitazone, or trolox, cell death was measured by lactate dehydrogenase (LDH) release into the conditioned media. Reactive oxygen species (ROS) formation was detected using a fluorescent ROS staining kit. Lysosomal integrity was assessed by LysoTracker staining. NF-κB activation was determined by immunostaining for nuclear translocation of NF-κB.

Results: Transfection with PPARγ siRNA achieved a significant reduction in the expression of PPARγ in ARPE-19 cells ($P < 0.001$). Treatment with troglitazone resulted in a significant decrease of oxLDL-induced LDH release, regardless of transfection with PPARγ siRNA or

scrambled siRNA ($P < 0.001$ for both conditions), whereas rosiglitazone did not. Treatment with oxLDL induced formation of reactive oxygen species (ROS) in ARPE-19 cells at 28 hours. Troglitazone and trolox, but not rosiglitazone, inhibited oxLDL-induced ROS formation. Furthermore, oxLDL treatment significantly decreased the number of intact lysosomes at 36 hours ($P < 0.05$). Treatment with troglitazone and trolox, but not rosiglitazone, significantly restored lysosomal integrity ($P < 0.05$ for troglitazone, $P < 0.001$ for trolox) in a dose-dependent manner. Finally, immunostaining revealed that oxLDL treatment induced NF-κB nuclear translocation at 36 hours. Troglitazone and trolox, but not rosiglitazone, inhibited NF-κB nuclear translocation in a dose-dependent manner.

Conclusions: These data suggest that troglitazone prevents oxLDL-induced ARPE-19 cytotoxicity, not through the PPARγ pathway, but rather through its antioxidant phenolic component, trolox. Troglitazone and trolox suppressed oxLDL-induced ROS formation, lysosomal destabilization, and NF-κB activation in ARPE-19 cells. Future direction of this research will investigate the link between oxidative stress and lysosomal integrity, investigate novel analogs of trolox their efficacy in protecting the RPE against oxLDL-induced cell death, and explore the efficacy of these drugs in a mouse model of dry AMD.

Glossary of Abbreviations

ABCA1: ATP-binding cassette, subfamily A, member 1

AGE: Advanced glycation end product

AMD: Age-related macular degeneration

APOE: Apolipoprotein E

AREDS: Age-related eye disease study

ARPE-19: Adult retinal pigment epithelium cell line-19

BHT: Butylated hydroxytoluene

CD36: Cluster of differentiation 36

CETP: Cholesteryl ester transfer protein

DAPI: 4′,6-diamidino-2-phenylindole

DMEM: Dulbecco's modified Eagle's medium

DMSO: Dimethyl sulfoxide

FBS: Fetal bovine serum

FITC: Fluorescein isothiocyanate

FLICA: Fluorescent-labeled inhibitor of caspase-1

Hf-RPE: Human fetal retinal pigment epithelium

HPRT1: Hypoxanthine phosphoribosyltransferase 1

IL-1β: Interleukin-1β

IκB: Nuclear factor of kappa light polypeptide gene enhancer in B-cells inhibitor

LDH: Lactate dehydrogenase

LIPC: Lipase C

NAC: N-acetylcysteine

NF-κB: Nuclear factor kappa-light-chain-enhancer of activated B cells

NLRP3: NLR family pyrin domain containing 3

OSE: Oxidation-specific epitope

OxLDL: Oxidized low-density lipoprotein

OxPL: Oxidized phospholipids

PBS: Phosphate-buffered saline

PMC: 2,2,5,7,8-pentamethyl-6-chromanol

POS: Photoreceptor outer segment

PPAR: Peroxisome proliferator-activated receptor

PUFA: Polyunsaturated fatty acid

ROS: Reactive oxygen species

RPE: Retinal pigment epithelium

RT-PCR: Real-time polymerase chain reaction

SiRNA: Silencing ribonucleic acid

tBH: tert-butyl hydroperoxide

TLR: Toll-like receptor

TNF-α: Tumor necrosis factor-α

TR: Targeted replacement

TZD: Thiazolidinedione

VEGF: Vascular endothelial growth factor

1. Introduction

1.1. Age-related macular degeneration

Age-related macular degeneration (AMD) is the leading cause of permanent vision loss in adults over 50 years of age, particularly in western industrialized countries.[1] AMD affects 8.7% of the worldwide population, and the prevalence of advanced AMD is projected to increase to 288 million by 2040.[2,3] AMD is characterized by the accumulation of insoluble drusen deposits in the retinal pigment epithelium (RPE) and in and around Bruch's membrane. There are two forms of advanced AMD: neovascular and dry. Neovascular (wet or exudative) AMD is associated with subretinal vessel growth and leakage, whereas dry (atrophic) AMD and its advanced form, geographic atrophy, is characterized by a progressive loss of the RPE, choriocapillaris and photoreceptor cells; both lead to central vision loss. Dry AMD accounts for 90% of all AMD cases. While wet AMD is the most damaging form, recent advances in treatment targeting VEGF have shown to slow disease progression and/or improve vision in the vast majority of patients.[4] On the other hand, development of treatment for dry AMD has not been as successful, and there is currently no definitive therapy available for this more prevalent form of disease. As the population ages, there is a clear need for developing an effective therapy for AMD. Understanding its pathogenesis will enable the design of targeted therapies not only to treat late-stage AMD but to prevent the disease at earlier stages.

1.2. Pathophysiology of AMD

The pathophysiology of AMD is largely unknown. It is believed to be caused by cumulative damage to the RPE with increasing age. The RPE is a monolayer of specialized epithelial cells attached to photoreceptor outer segments (POS) on the apical side and to Bruch's membrane on the basolateral side. The RPE performs several functions critical for maintaining

visual function, including transport of nutrients to the photoreceptors and phagocytosis of POS. In AMD, gradual degeneration of the RPE leads to atrophy of the underlying choriocapillaris and subsequent death of the overlying photoreceptors. Loss of photoreceptors in the macula, which contains predominantly light-sensitive cone cells, results in central vision loss. A number of genetic and environmental factors have been identified to play a role in the progression of AMD: broadly, these fall into the categories of aging, dysfunctional lipid metabolism, inflammation, and oxidative stress.[5]

1.3. Role of lipids

Lipids and lipoproteins that accumulate and become oxidized in Bruch's membrane and sub-RPE space are believed to be one of the key contributors to RPE dysfunction in AMD.[6,7] As mentioned earlier, the hallmark of AMD is the accumulation of drusen, which are made of a range of proteins, lipids, and lipid-carrying lipoproteins.[8,9] Drusen are the first clinically visible abnormality in early AMD and are associated with aging. Larger size and greater number of drusen are risk factors for advanced AMD.[10] Consistent with the notion that excess lipids may play a role in its pathogenesis, patients with AMD often have hyperlipidemia.[11] Progression of AMD is also associated with polymorphisms of genes related to lipid transport and metabolism, such as ABCA1, APOE, CETP, and LIPC.[12]

Studies have suggested that AMD and atherosclerosis share similarities in their pathogenesis. Drusen and atherosclerotic lesions both contain apolipoprotein B and cholesterol.[13] In atherosclerosis, cholesterol-transporting lipoproteins become retained in the subendothelium of arteries, and subsequent oxidative modifications can trigger pathologic responses that lead to coronary artery disease. Similarly, increased accumulation of oxidized lipids and carrier lipoprotein in the RPE cell layer and in Bruch's membrane is seen in human eyes with AMD and

has been suggested to contribute to the pathology.[6] As can be predicted by the mechanistic parallels between the two diseases, atherosclerosis has been correlated with AMD progression,[14] and cholesterol-lowering drugs may show a mildly protective effect against disease progression.[15–17] These findings suggest that lowering cholesterol levels and promoting lipid efflux may have a beneficial effect against AMD.

1.4. Role of oxidative stress

The retina is particularly susceptible to oxidative stress due to its high consumption of oxygen, relatively high concentration of polyunsaturated fatty acids (PUFAs), and abundant light exposure.[18] Furthermore, the RPE has unique sources of oxidative stress: phagocytosis of POS, during which intracellular H_2O_2 is generated by NADPH oxidase and β-oxidation of outer segment lipids, and photo-oxidative stress from light processing for vision.[19] These unique challenges, coupled with the decreasing antioxidant capacity of the macula with age, are thought to contribute to the development of AMD.[20] Also consistent with this notion is that cigarette smoking, which contains many chemical oxidants, is the strongest environmental risk factor for AMD.[21,22]

In addition, studies suggest a role for oxidized lipids and lysosomal dysfunction in the pathogenesis of AMD. Lipid peroxidation products disrupt the degradation of phagocytosed POS or cytoplasmic proteins in RPE cells, leading to long-term storage and accumulation of undigested material within lysosomes.[23,24] Lysosomal storage, in turn, leads to lipofuscin generation, which further increases oxidative stress and lysosomal dysfunction that causes damage to the RPE.

Finally, oxidative stress can induce an inflammatory response in the development of AMD. Inadequate neutralization of oxidative stress leads to oxidative modifications to proteins,

lipids, and DNA, which can generate oxidation-specific epitopes (OSEs).[19] These OSEs have pro-inflammatory effects *in vitro* and *in vivo*, and can activate both innate and adaptive immunity.[25,26] Multiple OSEs have been identified in the RPE and Bruch's membrane with drusen, including malondialdehyde (MDA), 4-hydroxynonenal (4-HNE), advanced glycation endproducts (AGEs), and oxidized phospholipids (OxPL).[27–29] While the initial response to these "danger signals" is intended to be cytoprotective, inadequate neutralization of OSEs can result in a pathologic response resulting in a chronic pro-inflammatory state. The link between oxidized lipids and inflammation is further discussed in the following section.

1.5. Role of inflammation

In addition to age-related changes such as increased lipid deposition and oxidative stress, inflammation is recognized as another important player in the pathogenesis of AMD.[30] Studies have implicated activation of the complement cascade as a major event underlying AMD progression. Drusen contain a number of proteins related to the complement pathway.[31] Furthermore, polymorphisms in certain complement pathway genes, such as complement factor H and C3, are strongly associated with AMD risk.[32–34]

Our lab and others have shown that the NLRP3 inflammasome, another component of the innate immune system, is activated in the RPE of human eyes with AMD.[35,36] The NLRP3 inflammasome is a multi-protein complex consisting of NLRP3, adaptor protein ASC, and procaspase-1, and serves as an intracellular sensor of metabolic stress. Upon activation, procaspase-1 is cleaved into active caspase-1, which catalyzes the proteolytic maturation of pro-inflammatory cytokines, pro-IL-1β and pro-IL-18, into mature IL-1β and IL-18, respectively.[37] Our lab has previously suggested a two-signal model of the NLRP3 inflammasome activation in RPE cells. Priming signals (signal 1), such as pro-inflammatory stimuli IL-1α and TNF-α,

activate nuclear transcription factor NF-κB, which upregulates the expression of pro-IL-1β and NLRP3. Lysosomal destabilization (signal 2), which may be induced by lipofuscin or drusen components, triggers inflammasome assembly by cytoplasmic release of lysosomal enzymes, cathepsins B and L. NLRP3 assembly activates caspase-1, which in turn induces IL-1β secretion and pyroptotic cell death (Figure 1).[35]

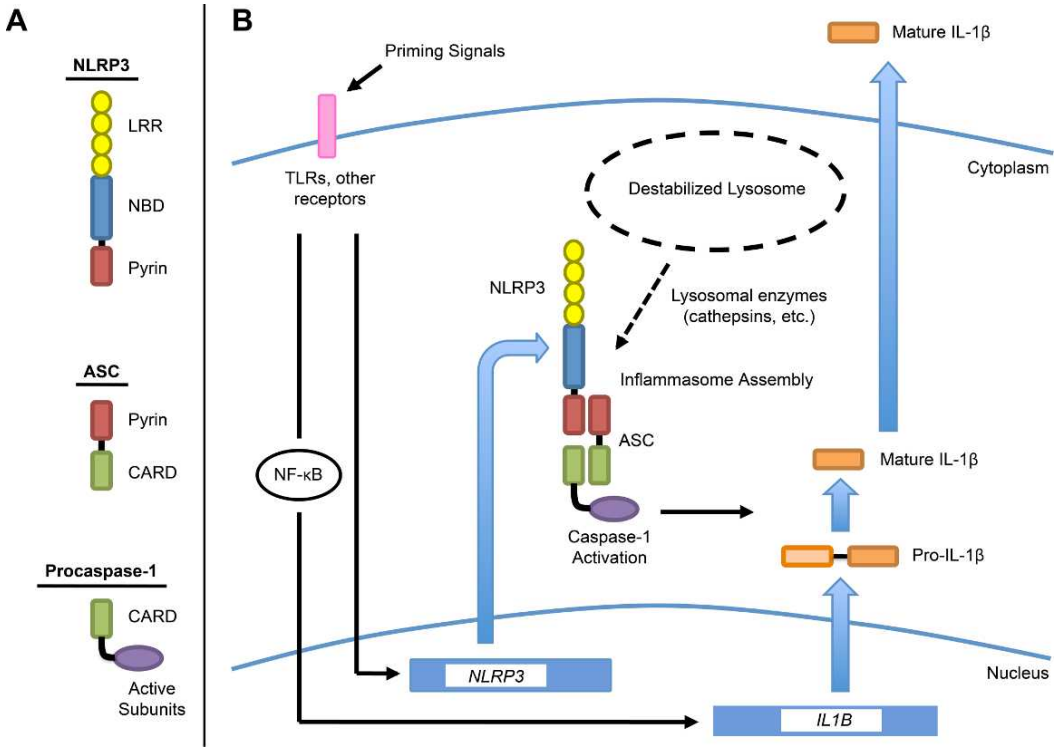

Figure 1. Proposed model of NLRP3 inflammasome activation in RPE cells by lysosomal destabilization.[35]

In macrophages, the NLRP3 inflammasome can be activated by a number of factors, including cholesterol crystals, amyloid-β, oxidized mitochondrial DNA, reactive oxygen species, and cell stress signals from the endoplasmic reticulum; many of these stimuli activate the inflammasome by destabilizing lysosomes.[38–41] Recently, our lab has shown that uptake of oxLDL leads to RPE cell death by lysosomal destabilization and activation of the NLRP3

inflammasome.[42] Internalization of oxLDL by the CD36 receptor on RPE cells results in lysosomal accumulation and destabilization, leading to NLRP3 inflammasome-mediated proinflammatory cytokine release and pyroptosis.[42] These findings suggest that promoting intracellular clearance of lipids would attenuate inflammation and RPE cell death.

1.6. Current therapeutic options

Many studies targeting the different possible pathologic mechanisms of dry AMD are being conducted. Currently, the recommended treatment for dry AMD in the United States is the AREDS2 formulation, based on two randomized clinical trials known as the Age-Related Eye Disease Study (AREDS). The first study found that for patients with intermediate AMD, daily oral high dose antioxidants (vitamin C, vitamin E, β-carotene, and copper) with zinc supplementation reduced the risk of developing advanced AMD by 25% at five years.[43] The second AREDS2 study found that addition of lutein and zeaxanthin (carotenoids) or omega-3 long-chain PUFAs did not further reduce the risk of progression to advanced AMD.[44] However, because of the higher incidence of lung cancer in the β-carotene group, the current recommendation is to substitute β-carotene with lutein and zeaxanthin in the AREDS formulation.

Antioxidants are not a universally accepted treatment, however. A meta-analysis of three large randomized clinical trials with over 23,000 patients showed that antioxidant supplementation did not prevent AMD.[45] In addition, certain components of the AREDS formulation may have potential adverse effects; for example, vitamin E was associated with a higher risk of heart failure in patients with vascular disease or diabetes,[46] and elevated zinc levels were associated with light-induced retinal neurodegeneration.[47]

There are ongoing clinical trials investigating complement pathway inhibitors as treatment for dry AMD. The most promising agent has been lampalizumab, a complement factor D inhibitor, which showed a significant reduction in the rate of geographic atrophy growth in phase 2 trials;[48] however, it failed to show any beneficial effects in phase 3 trials.[49] Taken together, despite the ongoing efforts to find a cure, there is currently a lack of definitive treatment of dry AMD. Thus, a search for novel therapeutic agents based on mechanistic studies is warranted.

1.7. Effect of PPARγ agonists on RPE integrity

Peroxisome proliferator-activated receptors (PPARα, β, δ, and γ) are nuclear receptors that regulate the expression of an array of genes involved in lipid metabolism and inflammation. In particular, PPARγ activates genes involved in reverse cholesterol transport and promotes the clearance of cellular cholesterol in animal models for atherosclerosis.[50] Furthermore, PPARγ suppresses inflammation by regulating the activity of inflammatory gene transcription factors NF-κB, NFAT, STAT, and AP-1 in macrophages.[50] These mechanisms may explain the protective role of PPARγ in atherosclerosis, which is also supported by a number of *in vivo* studies.[51]

Because of the role of PPARγ in suppressing inflammation and promoting lipid efflux, and the role of these pathways in the pathogenesis of AMD, we investigated whether pharmacologically activating PPARγ in RPE cells could protect against oxLDL-induced RPE degeneration. Our preliminary studies revealed that troglitazone, a PPARγ agonist, uniquely suppressed oxLDL-induced RPE cell death. Troglitazone is a member of the thiazolidinedione (TZD) class of drugs, initially used to treat patients with diabetes mellitus type 2. Its molecular

structure is composed of a TZD ring, thought to bind PPARγ, and an α-tocopherol moiety found in vitamin E with antioxidant activity.[52,53]

The purpose of this study is to elucidate the mechanism of troglitazone's protection of the RPE against ox-LDL induced cell death. We hypothesize that troglitazone, with its PPARγ-binding structure and phenolic ring, acts as both an anti-inflammatory and anti-oxidant agent to prevent oxLDL-induced cytotoxicity. To test our hypothesis, we first evaluated whether troglitazone acts through its proposed receptor, PPARγ. We then evaluated the role of troglitazone in suppressing oxLDL-induced oxidative stress, lysosomal destabilization, and NF-κB activation. The work reported here will provide insight into the mechanism of troglitazone and its therapeutic implications for dry AMD.

2. Methods

ARPE-19 Cell Culture

Human ARPE-19 cells were purchased from American Type Culture Collection (Manassas, VA). Cells were cultured in Dulbecco's modified Eagle's medium (DMEM)/F12 medium (Lonza, Walkersville, MD), supplemented with 10% fetal bovine serum (FBS; Atlanta Biologicals, Lawrenceville, GA) and 100 U/mL penicillin-100 μg/mL streptomycin (Lonza). Cells were incubated at 37°C in 5% CO_2 and passaged at a ratio of 1:2 to 1:4 with 1x trypsin-EDTA solution. Confluent monolayers of cells were maintained in media containing 1% FBS. For experiments, cells were maintained in serum-free medium overnight.

Lipoprotein and Drug Treatment

Troglitazone, rosiglitazone, and trolox were purchased from Cayman Chemicals (Ann Arbor, MI). Troglitazone and rosiglitazone stock solutions (33,975 μM) and trolox stock solution (67,950 μM) were prepared in DMSO. ARPE-19 cells, grown at postconfluence for 1 to 4 weeks, were serum-starved overnight and treated with oxLDL ± drug for various time points at 37°C. Treatment mixtures were prepared in serum-free media by suspending oxLDL (Biomedical Technologies, Alfa Aesar, LLC, Ward Hill, MA) to a final concentration of 200 μg/mL, then adding troglitazone, rosiglitazone, trolox, or DMSO vehicle to final concentrations ranging from 0.1625 μM to 10.4 μM. The drugs were serially diluted in DMSO so that the final DMSO concentration in cells was < 0.4 vol%. The controls received serum-free media containing the same amount of DMSO without oxLDL or drugs.

PPARγ Knockdown

Transfection mixtures were prepared as follows: PPARγ siRNA or non-targeting scrambled siRNA (ThermoFisher Scientific, Waltham, MA) was added to 100 uL of opti-MEM transfection media at a final concentration of 25, 50, and 100 nM. The target sequences of siRNAs are provided in the following table. Lipofectamine RNAiMAX reagent (ThermoFisher Scientific) was added, and the mixture was incubated for 30 minutes at room temperature. Meanwhile, ARPE-19 cells grown as described above were trypsinized and seeded into 24-well plates (VWR) at a density of 6.0 x 10^4 cells/well. Cells were then transfected with the prepared siRNA mixture and incubated at 37°C for 24 hours. Cell lysates were collected for RNA analysis.

For lipoprotein and drug treatment, cells were incubated with the transfection mixture for 16 hours, then with serum-free media for 8 hours. Twenty-four hours post-transfection, cells were treated with 200 μg/mL of oxLDL ± 1.3 μM of troglitazone or rosiglitazone for 48 hours. Conditioned media and cell lysates were collected for LDH assay and RNA analysis.

siRNA Pool	**Target Sequences**
PPARγ	No. 1: 5'-GGGCGAUCUUGACAGGAAtt-3'
	No. 2: 5'-UUUCCUGUCAAGAUCGCCCtc-3'

Assessment of Cell Death

The conditioned media were collected from ARPE-19 cells after 48 hours of treatment, and the percentage of cell death was quantified by measuring the release of lactate dehydrogenase (LDH) into the media using the CytoTox 96 Non-Radioactive Cytotoxicity Assay (Promega, Madison, WI). Maximum LDH release was measured from positive control cells that were maintained in parallel and lysed by two freeze–thaw cycles. The level of spontaneous LDH release was

measured from negative control cells that received no lipoprotein or drug treatment. Percentage LDH release was calculated as 100% × (experimental LDH − spontaneous LDH)/(maximum LDH − spontaneous LDH).

Real Time PCR (RT-PCR)

Total mRNA was purified using RNA-Bee solution (CS-105B; Amsbio, Cambridge, MA) under RNase-free conditions, according to the manufacturer's instructions. A total of 0.5 μg of RNA was reverse-transcribed using the iScript cDNA Synthesis Kit (Bio-Rad Laboratories, Hercules, CA), and the synthesized cDNA was diluted 1:10 (50 ng of equivalent RNA) for use in each amplification reaction. Real-time PCR reactions were performed using the SYBR Green master mix (Roche, Basel, Switzerland) and PCR platform (Light Cycler 480 II; Roche). PCR cycles consisted of an initial denaturation step at 95°C for 10 minutes, followed by 40 cycles of 95°C for 15 seconds and 60°C for 60 seconds. Each sample was subjected to melting curve analysis to confirm amplification specificity. Samples were run in duplicate, and relative gene expression, normalized to reference gene HPRT1, was calculated using the δ-delta Ct method. Primer sequences are provided in the following table.

Genes	**Forward Primer**	**Reverse Primer**
PPARg	5'-GGATTCAGCTGGTCGATATCAC-3'	5'-GTTTCAGAAATGCCTTGCAGT-3'
HPRT1	5'-GCGATGTCAATAGGACTCCAG-3'	5'-TTGTTGTAGGATATGCCCTTGA-3'

Detection of Reactive Oxygen Species (ROS)

Intracellular ROS were detected using the total ROS detection kit (Enzo Life Sciences, Farmingdale, NY) according to the manufacturer's instructions. ARPE-19 cells were seeded into

48-well plates at a density of 5.0 x 10^4 cells per well and maintained for 1-2 weeks. The cells were serum-starved overnight and treated with 100 μg/mL or 200 μg/mL of oxLDL for 6, 12, and 28 hours to determine the optimal parameters for ROS detection. At the end of the treatment period, cells were washed once with 1X wash buffer and stained with the ROS detection solution for 45 minutes at 37°C. After three washes in 1X wash buffer, cells were observed under a fluorescent microscope (EVOS FL Auto inverted microscope; Life Technologies), and images were taken of five randomly selected fields.

For lipoprotein and drug treatment, cells were serum-starved overnight and treated with 200 μg/mL of oxLDL in the presence or absence of troglitazone (1.3 μM), rosiglitazone (1.3 μM), or trolox (10.4 μM) for 28 hours. Intracellular ROS were detected as described above.

Assessment of Lysosomal Integrity

ARPE-19 cells were seeded on cover slips at a density of 7.5 x 10^4 cells per well and treated with oxLDL ± troglitazone, rosiglitazone, or trolox at various doses (0.16, 1.3, and 10.4 μM) for 18 and 36 hours. Cells were washed once with serum-free media without phenol red, then treated with 500 nM of LysoTracker Red DND-99 (Life Technologies, Carlsbad, CA) and Hoechst 33,342 nuclear stain (Immunochemistry Technologies, Bloomington, MN) to label the lysosomes and nucleus. After washing in serum-free media without phenol red, cells were fixed with 4% paraformaldehyde for 5 minutes. After three 10-minute washes in PBS, the cover slips were mounted onto slides using Prolong Gold Antifade Reagent (Life Technologies). Images were taken of five randomly selected fields using a fluorescent microscope (Axioscope Mot 2; Carl Zeiss Meditec, Inc., Dublin, CA) and analyzed using the ImageJ software

(http://imagej.nih.gov/ij/; provided in the public domain by the National Institutes of Health, Bethesda, MD) to quantify the number of intact lysosomal particles.

NF-κB Immunofluorescence

ARPE-19 cells were seeded on cover slips at a density of 7.5 x 10^4 cells per well and treated with oxLDL ± troglitazone, rosiglitazone, or trolox at various doses (0.16, 1.3, and 10.4 μM) for 18 and 36 hours. After washing with serum-free media, cells were fixed with 4% paraformaldehyde for 5 minutes and washed 3 times with PBS for 5 minutes each. Cells were then permeabilized with ice-cold 100% methanol for 2 minutes. After three 10-minute rinses in PBS, cells were blocked for 1 hour at room temperature in PBS containing 10% goat serum, 0.01% Triton X-100, and 0.01% sodium azide. Cells were then incubated overnight at 4°C in rabbit anti-NF-κB p65 primary antibody (Cell Signaling, Danvers, MA) diluted 1:400 in blocking solution that was diluted 4X in PBS. After three 10-minute washes in PBS, cells were incubated for 1.5 hours at room temperature in secondary antibody (Dylight 549 goat anti-rabbit IgG antibody; Vector Labs, Burlingame, CA) diluted 1:250 and DAPI nuclear stain (ThermoFisher) diluted 1:1000 in blocking buffer. After three 10-minute washes in PBS, the cover slips were mounted onto slides using Prolong Gold Antifade Reagent (Life Technologies). Images were taken of five randomly selected fields using a fluorescent microscope (Axioscope Mot 2; Carl Zeiss Meditec, Inc.) to assess for nuclear translocation of NF-κB.

Image Processing

Images taken of LysoTracker staining were processed using the ImageJ software (http://imagej.nih.gov/ij/) to better visualize intact lysosomal particles. First, the edges of the image were cropped to remove unfocused areas. After applying a median filter to remove noise,

the image was inverted, converted to 8-bit, and adjusted to a common threshold. Particles larger than 0 and smaller than 100 pixels were counted and normalized to the number of nuclei.

Statistical Analysis

Data are presented as the mean ± SEM of three independent experiments. To evaluate for statistical significance, one-way analysis of variance was performed, followed by the Tukey-Kramer multiple comparisons test using the Prism 6 software package (GraphPad, La Jolla, CA). A value of $P < 0.05$ was considered statistically significant.

3. Results

3.1. Mechanism of Troglitazone in its Protection of RPE Cells

Troglitazone, among other PPARγ agonists, uniquely protects against oxLDL-induced RPE cell death

(Credit: Eric Ng, PhD)

Preliminary work performed by Dr. Ng in the lab identified troglitazone as the only PPARγ agonist that significantly protected RPE cells from oxLDL-induced cell death. Treatment of ARPE-19 cells with 200 μg/mL of oxLDL for 48 hours induced significant LDH release (Fig. 2). Addition of various PPARγ agonists revealed that troglitazone significantly decreased LDH release in a dose-dependent manner, whereas other PPARγ agonists such as ciglitazone, rosiglitazone, and pioglitazone had no significant effect on LDH release ($P < 0.001$; Fig. 2).

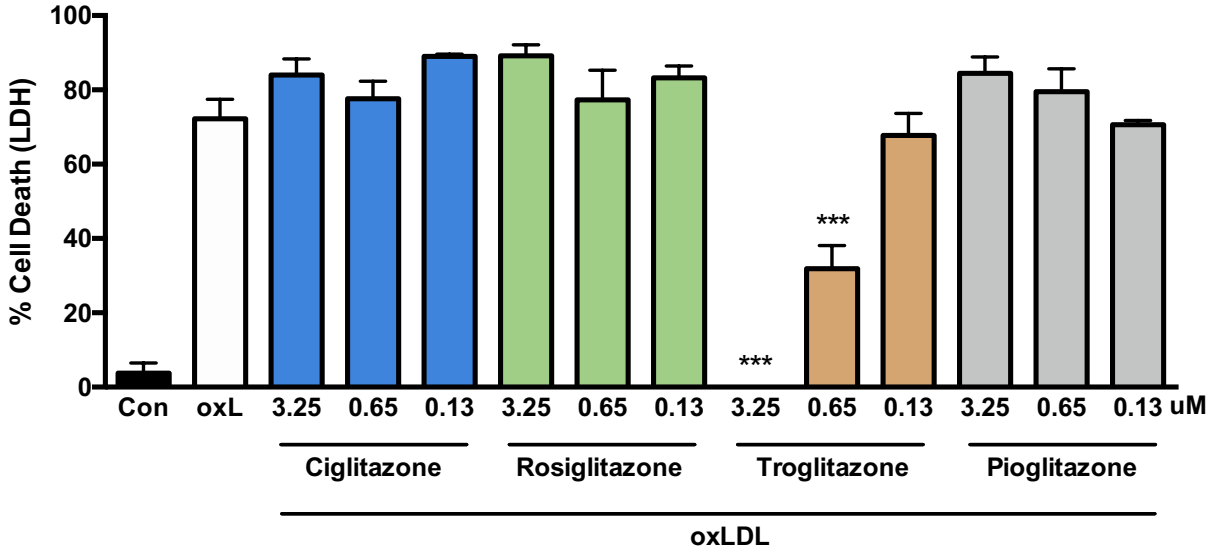

Figure 2. Profiles of various TZD PPARγ agonists. ARPE-19 cells were treated with oxLDL ± ciglitazone, rosiglitazone, troglitazone, and pioglitazone (3.25, 0.65, and 0.13 μM), and the conditioned media were collected to measure LDH release. % cell death was normalized to total cells in untreated control wells (100%). *** $P < 0.001$.

Troglitazone does not act through the PPARγ pathway to exert its effect against oxLDL-induced RPE cell death

The fact that only troglitazone significantly protected RPE cells from oxLDL-induced RPE cell death, and the other PPARγ agonists did not, suggested that troglitazone had a mechanism of action distinct from other PPARγ agonists. To determine whether the protective effect of troglitazone was dependent on its PPARγ activity, siRNA was used to knock down PPARγ in ARPE-19 cells. RT-PCR showed a significant decrease in PPARγ mRNA levels after transfection of ARPE-19 cells with 25, 50, and 100 nM of PPARγ siRNA, compared to transfection with scrambled siRNA (Fig. 3A; $P < 0.01$ for 25 nM, $P < 0.001$ for 50 nM and 100 nM), showing that the siRNA achieved the desired effect of inhibiting PPARγ expression. The following amounts of PPARγ knockdown were observed: 74% knockdown with 25 nM siRNA, 83% knockdown with 50 nM siRNA, and 89% knockdown with 100 nM siRNA. Based on these activities, 50 nM of PPARγ siRNA was chosen as the optimal concentration for additional studies.

After transfection with 50 nM of PPARγ siRNA, ARPE-19 cells were treated with 200 μg/mL of oxLDL ± 1.3 μM of troglitazone or rosiglitazone, and cell death was assessed using LDH assays. Even after PPARγ knockdown with siRNA, troglitazone treatment continued to result in a significant decrease in oxLDL-induced LDH release, whereas rosiglitazone treatment did not (Fig. 3B). The magnitude of reduction in LDH release with troglitazone after transfection with PPARγ siRNA was comparable to that with scrambled siRNA (Fig. 3B). Successful knockdown of PPARγ in the experimental conditions was confirmed with RT-PCR (Fig. 3C). Taken together, these data indicate that PPARγ activation is not a necessary component in the mechanism by which troglitazone protects against oxLDL-induced RPE cell death.

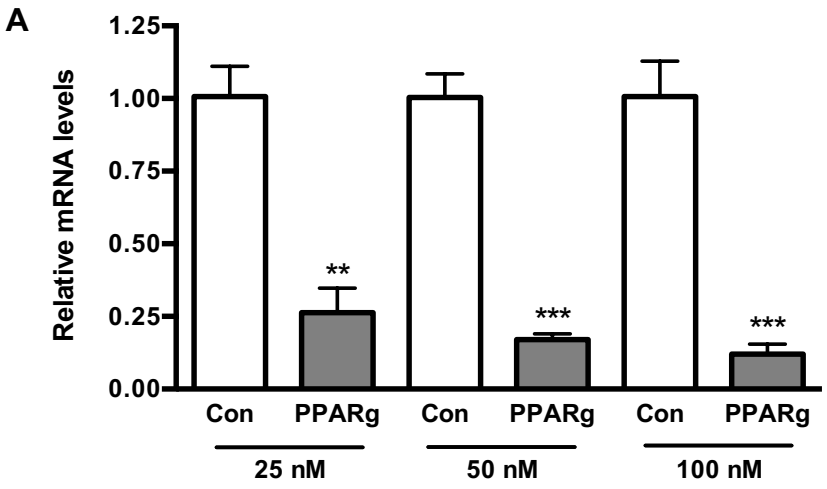
A
Relative mRNA levels
1.25
1.00
0.75
0.50
0.25
0.00
**
***
***
Con
PPARg
Con
PPARg
Con
PPARg
25 nM
50 nM
100 nM

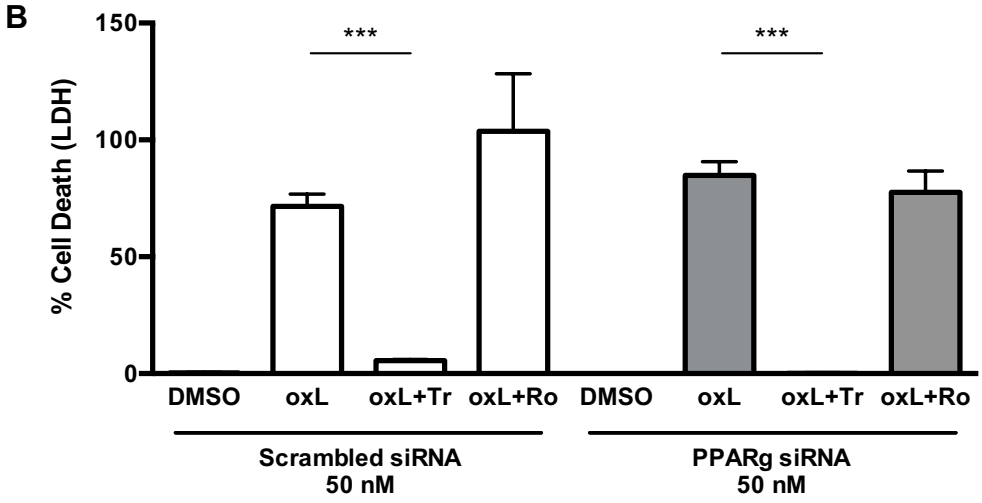
B
% Cell Death (LDH)
150
100
50
0
***
***
DMSO
oxL
oxL+Tr
oxL+Ro
DMSO
oxL
oxL+Tr
oxL+Ro
Scrambled siRNA
50 nM
PPARg siRNA
50 nM

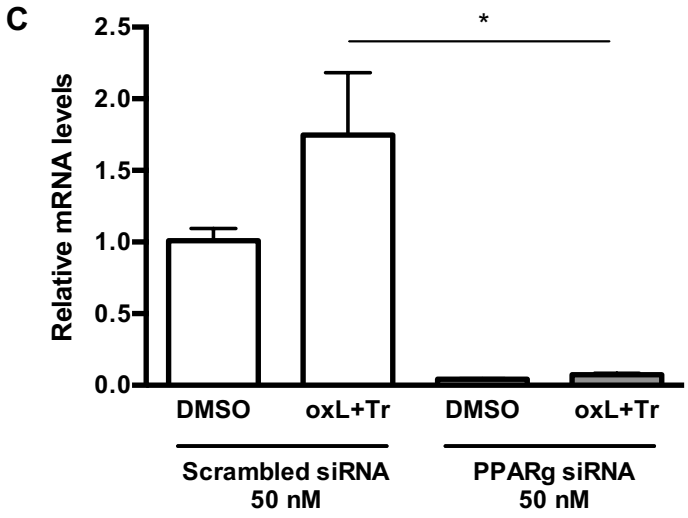
C
Relative mRNA levels
2.5
2.0
1.5
1.0
0.5
0.0
*
DMSO
oxL+Tr
DMSO
oxL+Tr
Scrambled siRNA
50 nM
PPARg siRNA
50 nM

Figure 3. PPARγ knockdown. **(A)** ARPE-19 cells were transfected with 25, 50, or 100 nM of siRNA against PPARγ or scrambled siRNA. After 24 hours, cell lysates were collected and PPARγ mRNA levels were analyzed by RT-PCR. **(B,C)** ARPE-19 cells were transfected with 50 nM of siRNA against PPARγ or scrambled siRNA for 16 hours, serum-starved for 8 hours, then treated with 200 μg/mL of oxLDL ± 1.3 μM of troglitazone or rosiglitazone for 48 hours. Conditioned media were collected to measure LDH release **(B)**, and cell lysates were collected to analyze PPARγ mRNA levels by RT-PCR **(C)**. *** $P < 0.001$, ** $P < 0.01$, * $P < 0.05$.

3.2. Effect on Reactive Oxygen Species

Having established that troglitazone protection of RPE is likely PPARγ-independent, we examined the structure of troglitazone in comparison to different PPARγ agonists. In addition to the thiazolidinedione ring that acts as the PPARγ binding group, troglitazone also contains an α-tocopherol moiety found in vitamin E, called trolox (6-hydroxy-2,5,7,8-tetramethylchroman-2-carboxylic acid), which acts as a phenolic antioxidant (Fig. 4A, 4C). The trolox component is unique to troglitazone and is not found in rosiglitazone (Fig. 4B) or other PPARγ agonists. We thus investigated whether trolox was responsible for troglitazone's protective effect, by testing if trolox by itself could suppress oxLDL-induced RPE cell death.

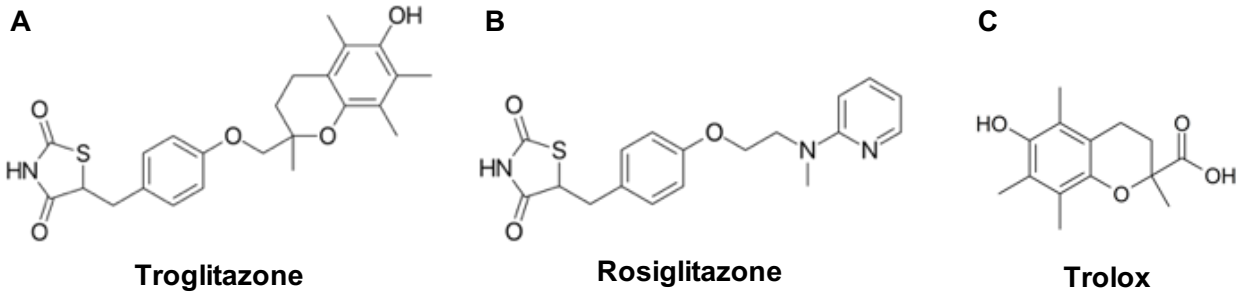

Figure 4. Chemical structures of (**A**) troglitazone, (**B**) rosiglitazone, and (**C**) trolox. Troglitazone contains an α-tocopherol moiety, whereas rosiglitazone does not.

Trolox dose-dependently suppresses oxLDL-induced RPE cell death

(Credit: Eric Ng, PhD)

To determine if trolox suppresses oxLDL-induced RPE cell death in a manner similar to troglitazone, ARPE-19 cells were treated with 200 μg/mL of oxLDL ± trolox or troglitazone at various doses for 48 hours, and LDH release was measured. Both trolox and troglitazone suppressed oxLDL-induced LDH release in a dose-dependent manner (Fig. 5). Trolox was less potent compared to troglitazone (EC50 for trolox = 5.436 μM; EC50 for troglitazone = 0.749 μM). Based on these findings, the 10.4 μM dose for trolox was selected for subsequent experiments.

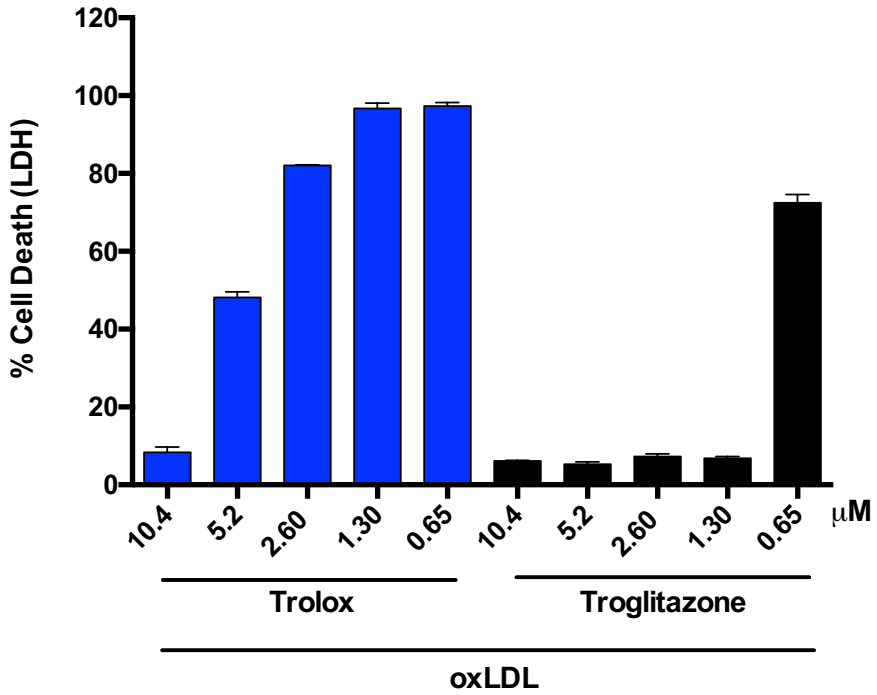

Figure 5. Profiles of trolox vs. troglitazone. ARPE-19 cells were treated with oxLDL ± trolox or troglitazone at various doses, and the conditioned media were collected to measure LDH release. % cell death was normalized to total cells in untreated control wells (100%).

OxLDL treatment leads to ROS formation in human RPE cells

Given that the antioxidant trolox alone was sufficient to suppress oxLDL-induced RPE cell death, we tested whether oxLDL induced ROS formation thus contributing to cytotoxicity in ARPE-19 cells. To investigate the time course of this process, ARPE-19 cells were treated with 200 μg/mL of oxLDL for 6, 12, and 28 hours. Induction of intracellular ROS was detected in oxLDL-treated cells at 28 hours, but not at earlier time points (Fig. 6).

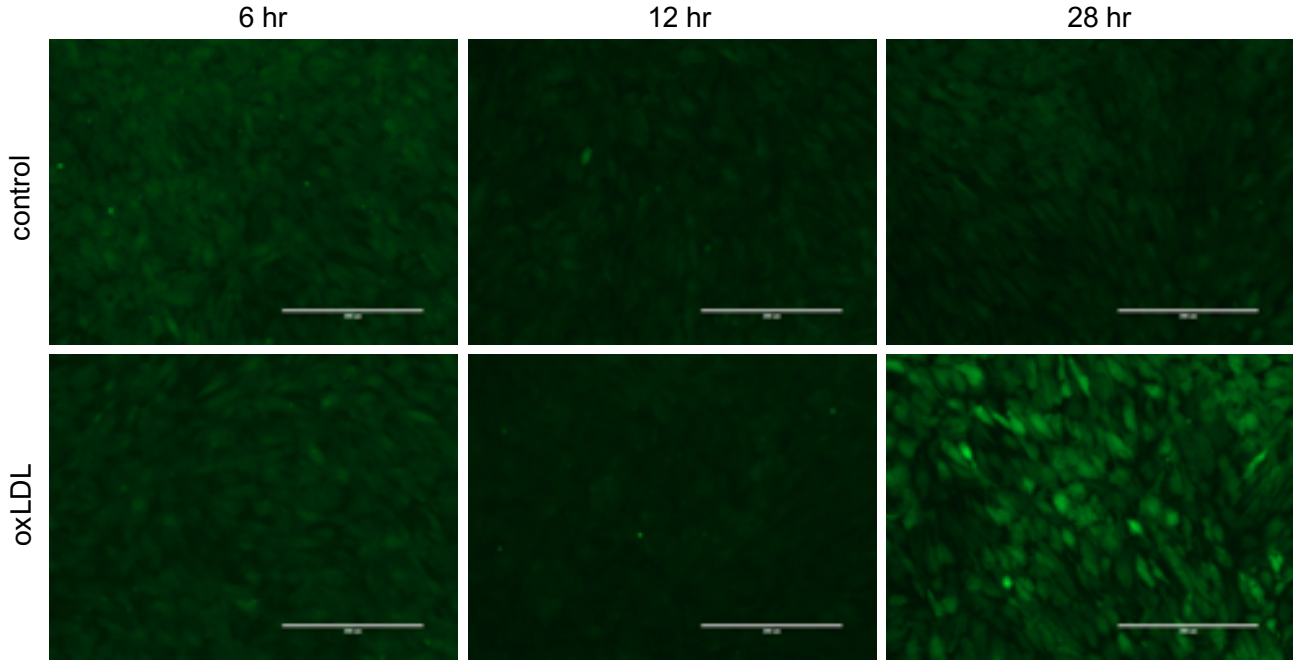

Figure 6. OxLDL leads to ROS formation at 28 hours. ARPE-19 cells were treated with 200 μg/mL of oxLDL for 6, 12, and 28 hours. After staining with the ROS detection solution for 45 minutes, intracellular ROS were detected using a fluorescent microscope. *Scale bars*, 200 μm.

Troglitazone and trolox, but not rosiglitazone, suppresses oxLDL-induced ROS formation

To determine the effect of the drugs on oxLDL-induced ROS formation, ARPE-19 cells were treated with 200 μg/mL of oxLDL ± troglitazone (1.3 μM), rosiglitazone (1.3 μM), or trolox (10.4 μM) for 28 hours. Intracellular ROS was detected using a fluorescent ROS detection solution. Treatment with oxLDL alone resulted in induction of ROS formation at 28 hours (Fig. 7). Troglitazone and trolox almost entirely suppressed oxLDL-induced ROS formation, while rosiglitazone resulted in only a mild reduction of ROS formation (Fig. 7).

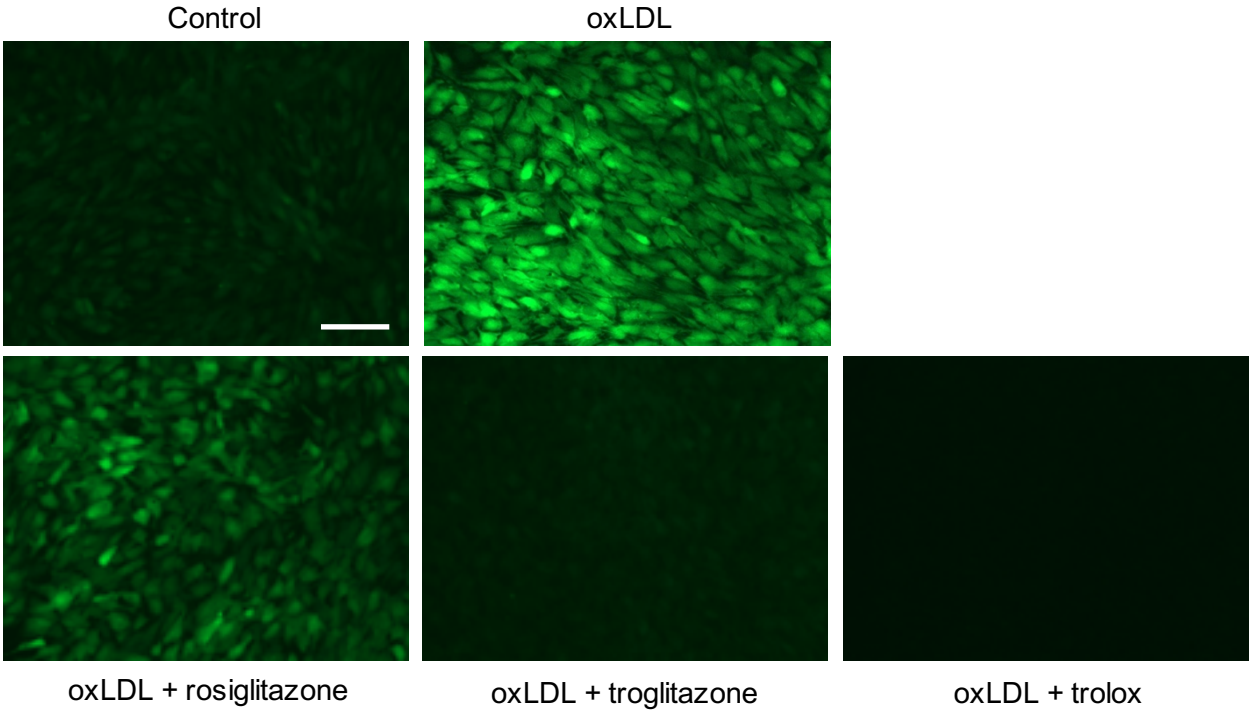

Figure 7. Troglitazone and trolox, but not rosiglitazone, leads to a dramatic reduction in oxLDL-induced ROS formation. ARPE-19 cells were treated with 200 μg/mL of oxLDL ± troglitazone (1.3 μM), rosiglitazone (1.3 μM), or trolox (10.4 μM) for 28 hours. After staining with the ROS detection solution for 45 minutes, intracellular ROS were detected using a fluorescent microscope. *Scale bar*, 100 μm. Results are representative of three independent experiments.

3.3. Effect on Inflammation

Troglitazone and trolox, but not rosiglitazone, suppress oxLDL-induced lysosomal destabilization

Previously, our lab has demonstrated that RPE cells exposed to oxLDL, but not LDL, exhibited lysosomal destabilization, NLRP3 inflammasome activation, and inflammatory cytokine release.[42] It was also shown that oxLDL is targeted to lysosomes through the CD36 receptor,[42] and the accumulation of oxLDL in lysosomes can generate lipofuscin and cause cellular dysfunction.[23,24] Given these findings and the antioxidant properties of troglitazone and trolox, we investigated whether these drugs could suppress oxLDL-induced lysosomal destabilization. Lysosomal integrity was assessed using the LysoTracker DND-99 dye which stains acidic organelles within cells, and the number of intact lysosomes was quantified using ImageJ.

Treatment with 200 μg/mL of oxLDL resulted in a significant decrease in lysosomal staining at 36 hours (Fig. 8A, 8C; $P < 0.05$). The addition of troglitazone at higher doses (10.4 μM and 1.3 μM) significantly increased lysosomal staining at 36 hours, restoring the number of intact lysosomal particles above the baseline (Fig. 8A, 8C; $P < 0.05$). The same was true for trolox at the highest dose (10.4 μM), but not at lower doses (Fig. 8A, 8C; $P < 0.001$). Treatment with rosiglitazone failed to reverse the loss of intact lysosomal particles. There were no significant changes in the level of lysosomes at 18 hours across all conditions (Fig. 8B). These data, taken together, provide evidence that oxLDL induced lysosomal destabilization in ARPE-19 cells at 36 hours, and co-treatment with troglitazone or trolox, but not rosiglitazone, preserved lysosomal integrity in a dose-dependent manner.

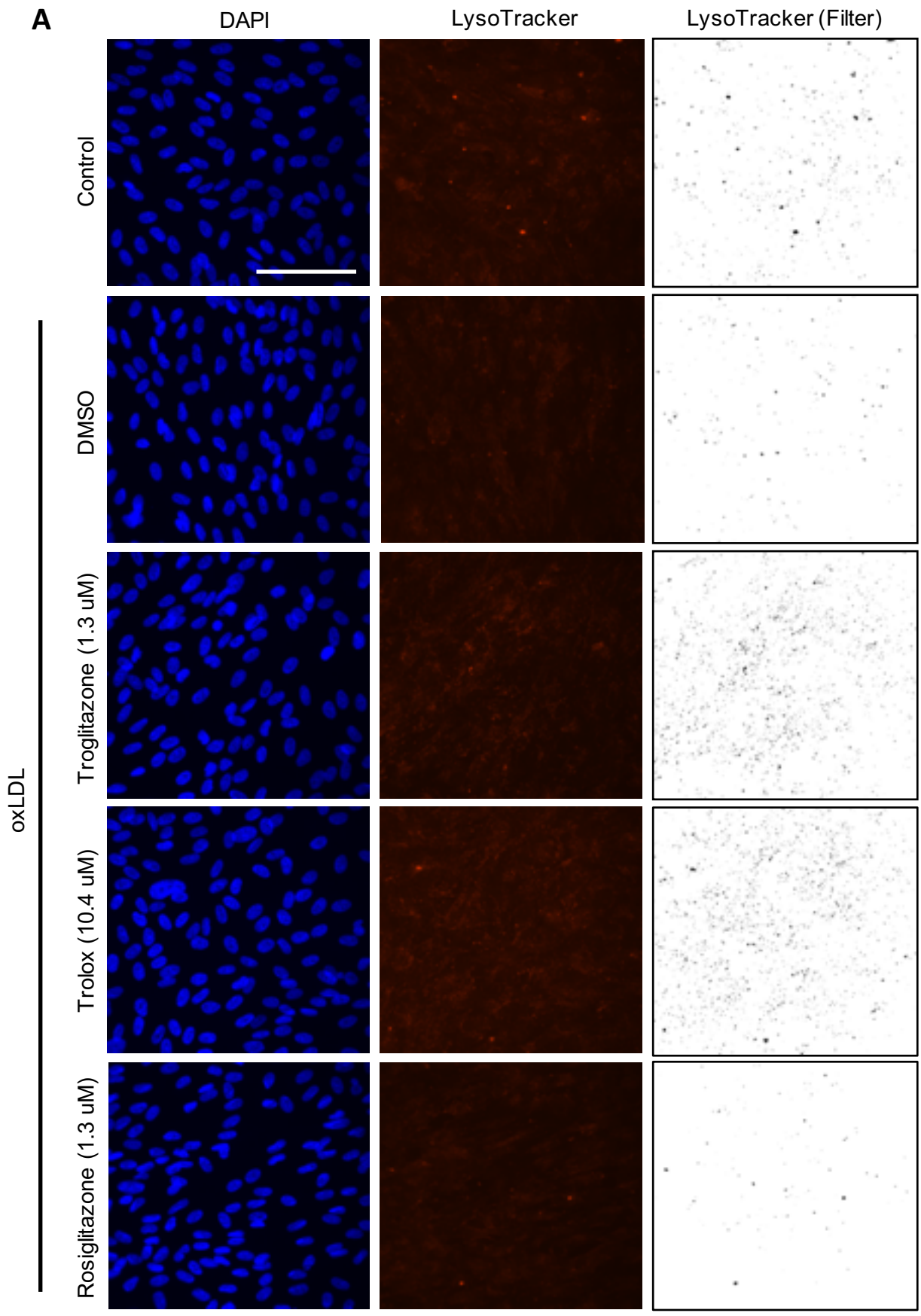
A
DAPI
LysoTracker
LysoTracker (Filter)
Control
DMSO
Troglitazone (1.3 uM)
Trolox (10.4 uM)
Rosiglitazone (1.3 uM)
oxLDL

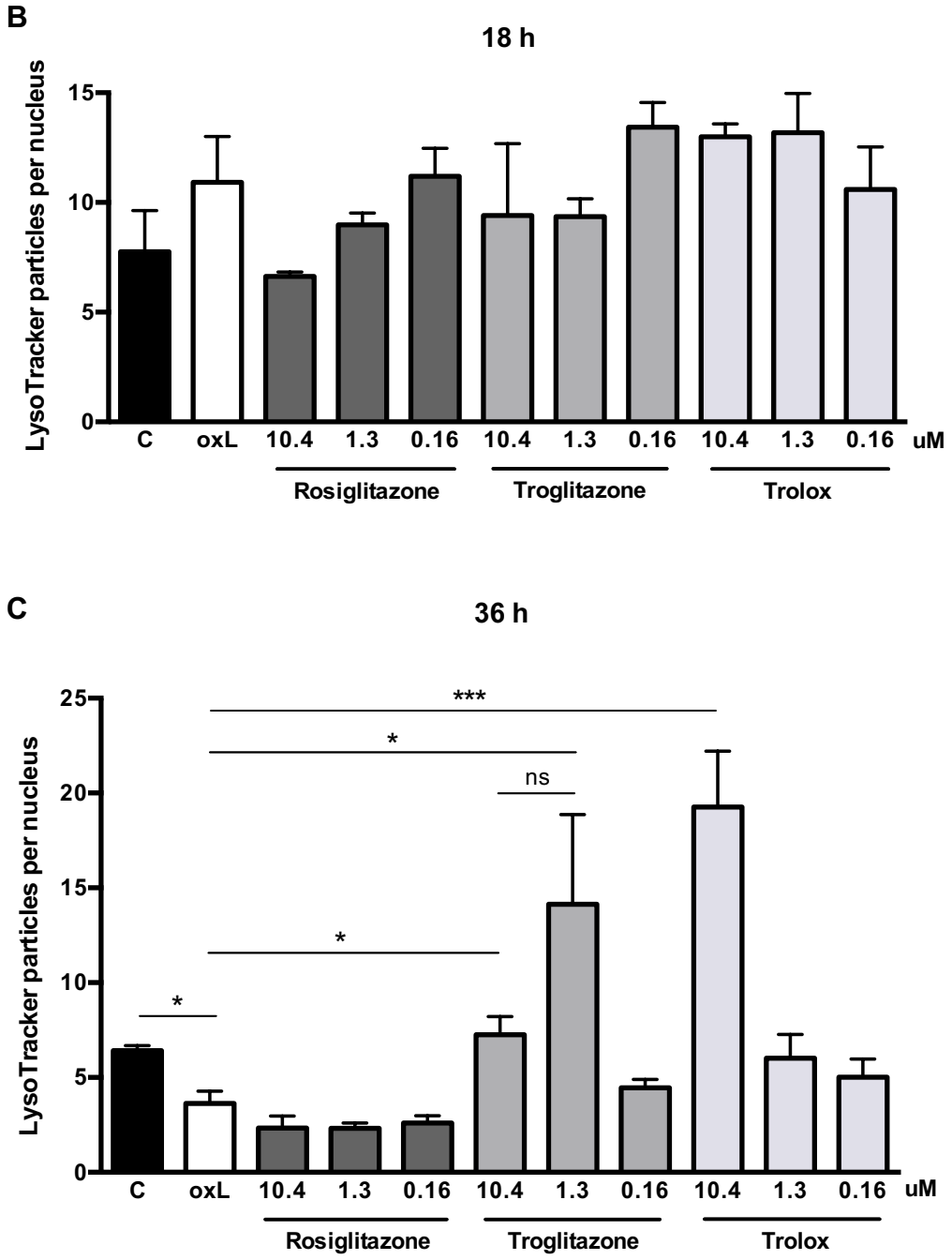

Figure 8. Troglitazone and trolox, but not rosiglitazone, suppresses oxLDL-induced lysosomal destabilization. (**A**) ARPE-19 cells grown on cover slips were treated with 200 μg/mL of oxLDL ± troglitazone, trolox, or rosiglitazone (0.16, 1.3, and 10.4 μM) for 18 and 36 hours (only data for 36 h shown). Prior to fixation, cells were stained with LysoTracker DND-99 (red) and Hoechst 33,342 (blue). Fluorescent microscopy was used to detect intact lysosomes (red) and nuclei (blue), and images were processed on ImageJ for better visualization of lysosomal particles. Representative images are shown. *Scale bars*, 100 μm. (**B, C**) Intact lysosomal particles were quantified using ImageJ and normalized to the number of nuclei (n = 3). * $P < 0.05$, *** $P < 0.001$.

Troglitazone and trolox, but not rosiglitazone, suppress oxLDL-induced NF-κB activation

Previous studies have shown that oxLDL induces activation of NF-κB via the CD36-TLR4-TLR6 pathway,[56] and that NF-κB is a required signal for priming the NLRP3 inflammasome in macrophages.[57] Furthermore, there is evidence that oxidative stress can activate innate immunity via oxidation-specific epitopes.[25] Given these findings, we investigated whether troglitazone and trolox could suppress oxLDL-induced NF-κB activation.

First, to examine the time course of NF-κB activation with oxLDL, ARPE-19 cells were treated with 200 μg/mL of oxLDL for 18 and 36 hours, and stained with an antibody against NF-κB and a nuclear dye. In the control samples, NF-κB (red) was localized mostly to the cytosol. In contrast, cells treated with oxLDL for 36 hours showed marked nuclear translocation of NF-κB, with the staining strongest in the peri-nuclear regions (Fig. 9A). No changes were seen after treatment with oxLDL for 18 hours. These data indicate that at 36 hours, oxLDL strongly induces NF-κB activation in RPE cells.

Next, to investigate the effect of the drugs on oxLDL-induced NF-kB activation, ARPE-19 cells were treated with 200 μg/mL of oxLDL ± troglitazone, rosiglitazone, or trolox at various doses for 36 hours, and stained with an antibody against NF-κB (Fig. 9B). Nuclear translocation of NF-κB was observed after treatment with oxLDL alone, as seen previously. With the addition of troglitazone, nuclear translocation of NF-κB occurred at the lowest dose (0.16 μM), but not at higher doses (1.3 μM and 10.4 μM). With the addition of trolox, nuclear translocation of NF-κB occurred at the lower doses (0.16 μM and 1.3 μM), but not at the highest dose (10.4 μM). Rosiglitazone failed to prevent nuclear translocation at all three doses. These data indicate that troglitazone and trolox dose-dependently suppress oxLDL-induced NF-κB activation, whereas rosiglitazone does not.

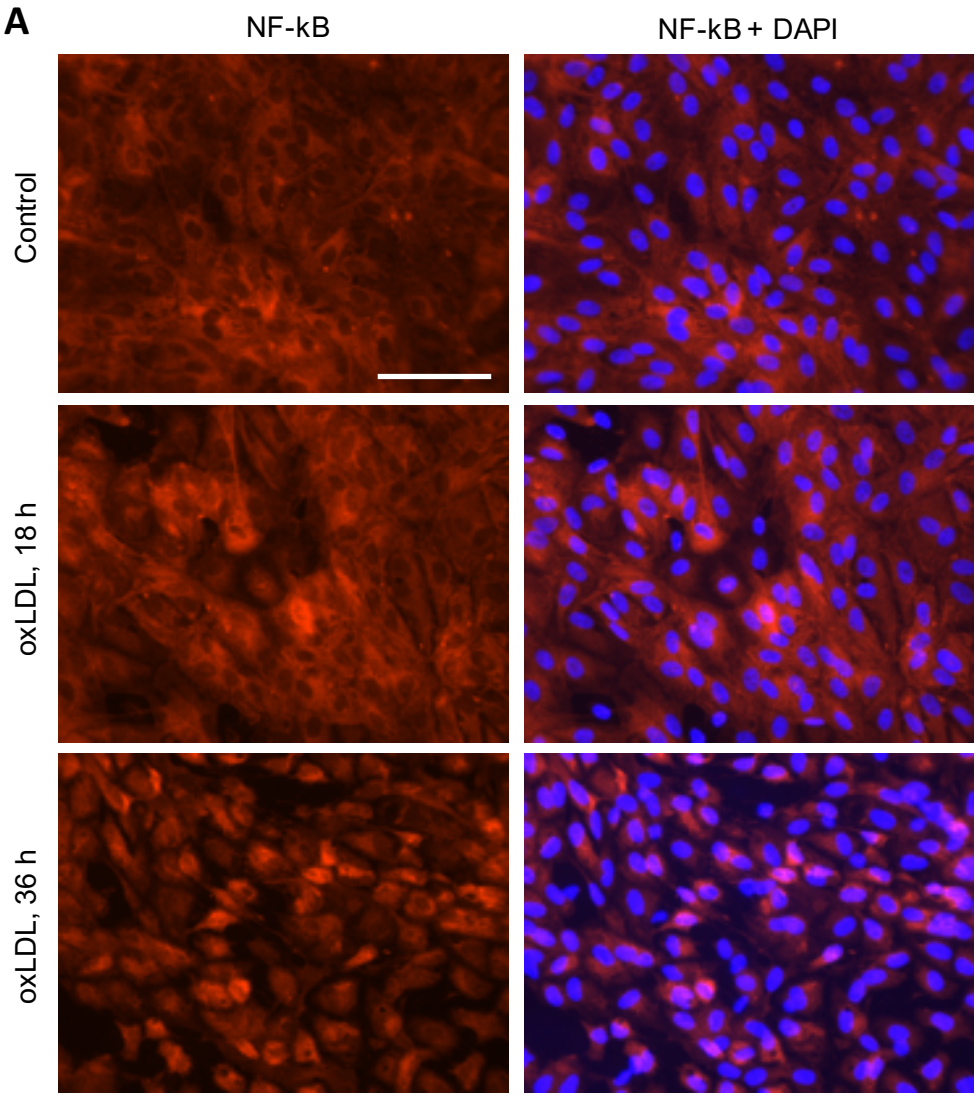
A
NF-kB
NF-kB + DAPI
Control
oxLDL, 18 h
oxLDL, 36 h

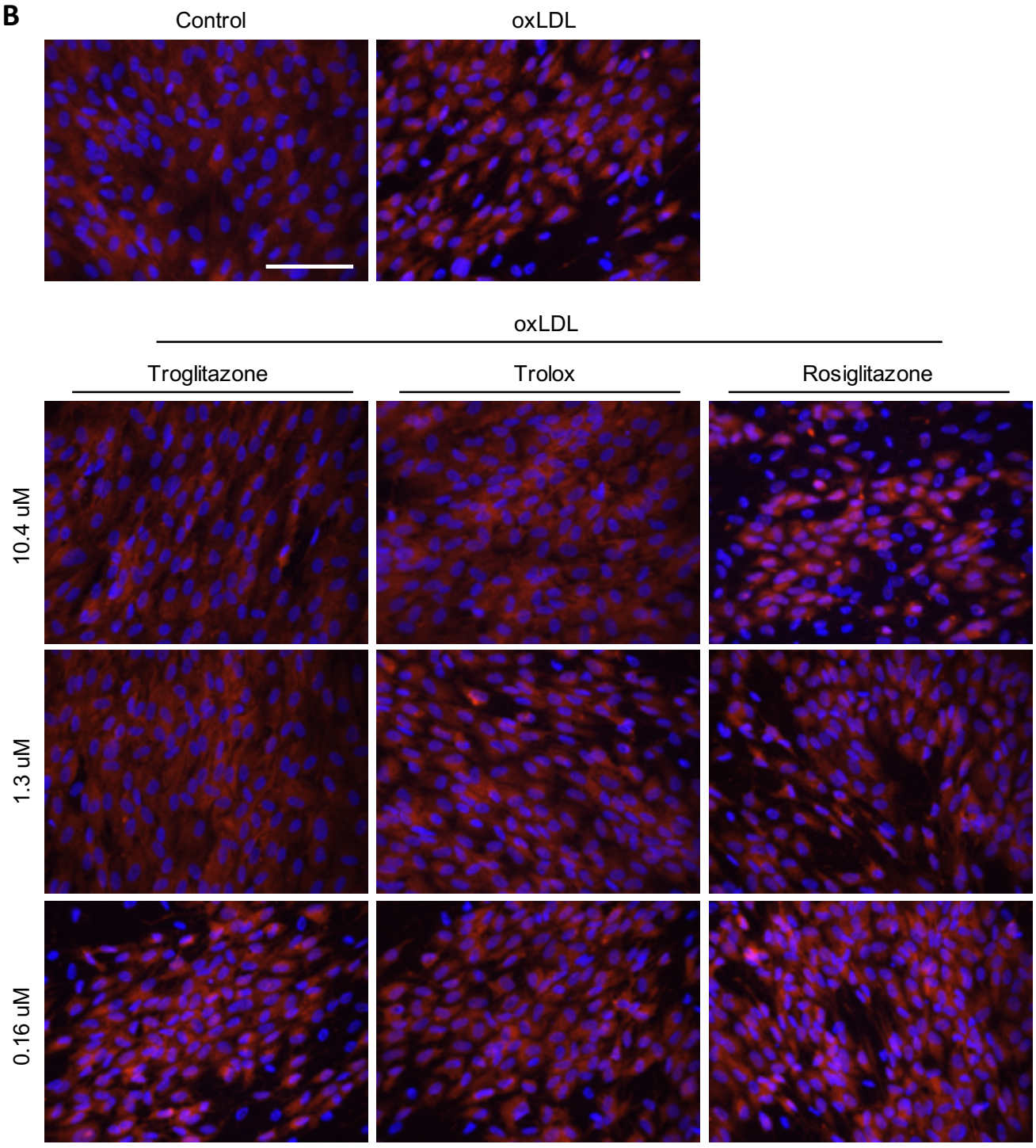

Figure 9. Troglitazone and trolox, but not rosiglitazone, suppresses oxLDL-induced NF-κB nuclear translocation at 36 hours. ARPE-19 cells were grown on cover slips and treated with 200 μg/mL of oxLDL for 18 and 36 hours (**A**), and with oxLDL ± troglitazone, trolox, or rosiglitazone (0.16, 1.3, and 10.4 μM) for 36 hours (**B**). Cells were fixed, permeabilized, and stained for NF-κB (red) and with DAPI (blue) to reveal nuclei. *Scale bars*, 100 μm.

4. Discussion

The pathogenesis of dry AMD is complex. Dysfunctional lipid metabolism, oxidative stress, and inflammation are thought to be the key elements of its pathogenesis. Many potential therapeutics targeting these individual pathways have been investigated in recent years with limited success. Here, we demonstrate that phenolic antioxidants, troglitazone and trolox, protect RPE cells from oxLDL-induced damage by suppressing ROS generation, NF-κB activation and lysosomal destabilization.

PPARs are ligand-activated transcription factors that increase lipid metabolism and suppress inflammation. Given the theoretical benefit of activating PPAR, we first focused our attention on PPAR agonists. Among various PPARγ agonists tested, only troglitazone showed significant efficacy in protecting the RPE from oxLDL-induced cell death (Fig. 2). This was in agreement with a previous study showing that troglitazone, but not other TZDs, protected RPE cells from oxidative stress.[58] Motivated by the unique therapeutic potential of troglitazone, we studied its mechanism of action in protecting the RPE. Surprisingly, we observed that troglitazone had the same protective effect even after knockdown of PPARγ with siRNA (Fig. 3), suggesting that it acted independently of PPARγ. Interestingly, this result was in contrast to Rodrigues *et al*. which showed that troglitazone's cytoprotective effect after exposure to oxidative stress was PPARγ-dependent.[58] This discrepancy is likely due to their use of t-butyl hydroperoxide (tBH) to induce oxidative stress. tBH, similar to H_2O_2, kills cells within hours and damages all cellular organelles, whereas oxLDL goes through a receptor-mediated pathway and kills cells in a time-dependent manner. Therefore, oxLDL is much more physiologically relevant than tBH as a toxic stimulation model. In addition, their study did not include scrambled siRNA but rather used untransfected (naïve) cells as a control, making the interpretation of their results difficult. The fact that other PPARγ agonists were not protective, and that trolox, the vitamin E-

like antioxidant component of troglitazone which does not bind PPARγ (Fig. 4), exhibited similar protection by itself (Fig. 5), further supports our hypothesis that the effect is independent of PPARγ. This is consistent with a number of studies which have shown that troglitazone acts independently of PPARγ to exert anti-tumor effects. Troglitazone decreased c-Myc expression in prostate cancer cells,[59] suppressed growth and promoted apoptosis in colon cancer cells,[60] and inhibited glioma cell migration and brain invasion,[61] all in a PPARγ-independent manner. Taken together, these data suggest that troglitazone is capable of regulating protein expression and cellular function in a PPARγ-independent manner across different cell types.

With evidence that troglitazone's effect was distinct from the PPARγ pathway, and that trolox also exhibited similar cytoprotection, we hypothesized that these effects were secondary to their antioxidant properties. OxLDL has previously been shown to induce ROS formation in vascular endothelial cells, leading to atherosclerosis,[62] and RPE cells in contact with oxysterols have been shown to display increased ROS content.[63] Furthermore, there are numerous reports of vitamin E analogs, such as troglitazone and trolox, acting to reduce ROS formation in various cell types.[64,65] As expected, our study showed that treatment with oxLDL led to ROS formation in ARPE-19 cells (Fig. 6), and that troglitazone and trolox dramatically suppressed oxLDL-induced ROS formation (Fig. 7). These results support our hypothesis that troglitazone and trolox function as antioxidants and mitigate the oxidative stress caused by oxLDL, thus protecting RPE cells.

Next, we examined the relationship between oxidative stress and lysosomal integrity. Studies suggest that oxidative stress can lead to lysosomal dysfunction via lipid peroxidation products.[23,24,66] Our lab has also previously shown that oxLDL localizes to lysosomes following cellular uptake and induces lysosomal destabilization in ARPE-19 cells.[42] We investigated whether troglitazone and trolox, by suppressing ROS formation, could also suppress lysosomal

destabilization. Our results show that troglitazone and trolox significantly increased the number of intact lysosomes after oxLDL treatment, as measured by LysoTracker staining (Fig. 8). The lack of effect with rosiglitazone indicates that the antioxidant property is necessary for lysosomal protection. This is consistent with a previous study demonstrating that inhibition of lipid peroxidation with trolox preserved lysosomal integrity in rat hepatocytes.[67] Taken together, these data suggest that by preventing ROS formation, troglitazone and trolox stabilize lysosomes and prevent RPE damage.

Interestingly, LysoTracker staining after treatment with troglitazone (1.3 μM) and trolox (10.4 μM) was increased above the level of the control, i.e. the baseline. This is likely due to the fact that the LysoTracker assay measures the number of lysosomal particles without taking size into consideration, and therefore may not be very accurate. Some particles may clump, artificially lowering the number of intact lysosomes, and smaller particles may have been detected in troglitazone- and trolox-treated cells. It should also be noted that for quantification, the size range of particles counted as a single lysosome was rather large (between 0 and 100 pixels).

The exact mechanism by which these compounds protect lysosomal integrity is yet to be determined. Preliminary data from our lab, using a fluorescein isothiocyanate (FITC) conjugated with trolox, showed that FITC-trolox localizes to potential membrane organelles in ARPE-19 cells (data not shown). These results are particularly interesting as they suggest a possible role of trolox as an antioxidant that acts directly on lysosomal and/or mitochondrial membranes, preventing lysosomal damage by ROS.

Using immunostaining, we also show that exposure to oxLDL induces nuclear translocation of NF-κB in ARPE-19 cells, and that treatment with troglitazone or trolox suppresses this effect (Fig. 9). NF-κB is a transcription factor that, when activated, dissociates

from its cytoplasmic inhibitor IκB as it gets degraded, and translocates to the nucleus. These results are consistent with previous reports showing that oxidative stress leads to NF-κB activation, and that various antioxidants inhibit NF-κB activation in cells stimulated with cytokines or LPS.[68–70] There is also evidence that PPAR agonists inhibit the DNA binding of NF-κB and thus suppress its signaling pathway.[71,72] However, the fact that troglitazone and trolox both suppressed NF-κB and rosiglitazone did not, indicates that the antioxidant property, not PPARγ activity, was responsible for suppressing NF-κB activation.

Our lab and others have implicated a role for the NLRP3 inflammasome in the pathogenesis of dry AMD.[35,36] Current literature suggests a 2-signal model in the activation of the inflammasome: a "priming" signal, such as toll-like receptors (TLRs), and a second signal that causes lysosomal destabilization. The priming signal activates NF-κB and induces release of pro-IL-1β. Lysosomal destabilization acts as the second signal which leads to aggregation of insoluble materials and induces cytosolic release of lysosomal contents or ROS formation. Together, these signals result in the activation of inflammasome assembly.[35,38] Our lab has previously shown that oxLDL induces NLRP3 inflammasome activation and inflammatory cytokine release in RPE cells.[42] Although the current study did not specifically investigate NLRP3 inflammasome activation, our data are consistent with the notion that troglitazone and trolox inhibit both signals 1 and 2, thereby potentially inhibiting subsequent inflammasome activation and cell death.

The observations from this study, in the context of current literature, point to the following sequence of events in AMD pathogenesis: 1) lipid accumulation and oxidation, 2) ROS formation, 3) lysosomal destabilization, 4) NF-κB activation, 5) NLRP3 inflammasome activation, and 6) RPE cell death (Fig. 10). It is unclear whether troglitazone and trolox are

capable of suppressing each of these steps, or whether their inhibition of ROS formation leads to downstream suppression of the subsequent steps. Further work remains to be done to elucidate the pathway in more detail. Regardless, our findings support the multi-dimensional role of troglitazone and trolox as antioxidants and anti-inflammatory agents that protect lysosomal integrity.

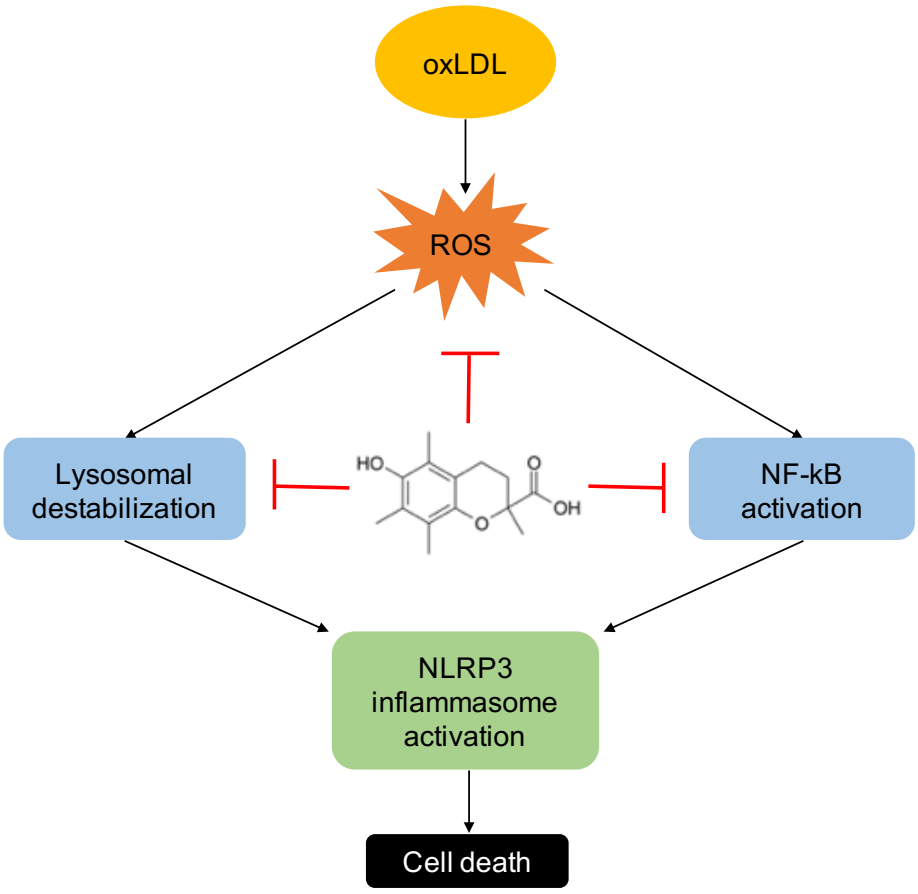

Figure 10. Schematic diagram representing the proposed model of AMD pathogenesis in RPE cells. Lipids accumulate and are then oxidized, leading to ROS formation, which then induce lysosomal destabilization and NF-κB activation. These two signals lead to NLRP3 inflammasome activation and eventual cell death. Trolox (shown in the center) and other related phenolic antioxidants are thought to target this pathway.

Of particular interest is the therapeutic potential of troglitazone and trolox for dry AMD. Given their ability to target multiple key pathways in AMD pathogenesis, they represent promising solutions to preventing RPE degeneration. Notably, the identification of these compounds and their mechanism of action has led to the screening of related antioxidants for enhanced efficacy. Ongoing efforts in the lab have identified several compounds containing a "hindered phenol" group, such as butylated hydroxytoluene (BHT) and 2,2,5,7,8-pentamethyl-6-chromanol (PMC), which were more effective than trolox or troglitazone. This is consistent with a previous study showing that PMC is the most effective antioxidant of the vitamin E analogs and could have a therapeutic advantage over others.[73] Compared to other common antioxidants such as N-acetylcysteine (NAC), hindered phenol compounds are uniquely effective at protecting RPE cells from oxLDL induced damage by an unknown mechanism, potentially through lysosomal membrane stabilization.

Limitations

There are several limitations of this study. First, in the PPARγ knockdown study, reduction in the mRNA levels after transfection with siRNA was confirmed with RT-PCR (Fig. 3). However, to demonstrate knockdown of actual protein expression, immunoblotting for PPARγ protein could be performed. Likewise, in the NF-κB activation study, immunostaining was used to demonstrate nuclear translocation of NF-κB (Fig. 9). This could be confirmed with immunoblotting for IκB-α, which gets degraded with NF-κB activation, and correlating the levels of IκB degradation with NF-κB nuclear translocation. To further support the activation of NF-κB, pro-IL-1β or IL-1β expression could be measured with immunoblotting. It should be noted that Western blots for PPARγ and IκB-α were attempted, however due to technical

difficulties and time constraints, it was determined that the results could not be interpreted reliably and thus were excluded this thesis.

Additionally, NLRP3 inflammasome activation could be evaluated using the fluorescent-labeled inhibitor of caspase-1 (FLICA) assay to detect active caspase-1. For the ROS assay, the Enzo total ROS detection kit detects hydrogen peroxide, peroxynitrite, and hydroxyl radicals, but not superoxide. More specific assays could be performed to look for certain ROS, and the fluorescent signal could be quantified to measure significance.

Finally, only ARPE-19 cells were used for the experiments in this study. The ARPE-19 cell line is commercially available and has been widely used to study RPE function. Primary human fetal RPE (hf-RPE) cells are more difficult to culture and maintain but may serve as a better model of native RPE function in vivo compared to ARPE-19 cells.[74] Thus, performing experiments in both ARPE-19 and primary hf-RPE cells would make the findings more biologically robust.

Conclusion and Future Directions

In conclusion, our work shows that PPARγ agonist troglitazone acts independently of PPARγ to protect RPE cells from oxLDL-induced cytotoxicity. Rather, it acts as an antioxidant to suppress oxLDL-induced ROS formation, lysosomal destabilization, and NF-κB activation. These effects were also seen in trolox, demonstrating that the phenolic antioxidant property is key to its downstream cytoprotective effects. By targeting multiple mechanisms involved in the pathogenesis of AMD, phenolic antioxidants show promise as potential therapeutic agents for dry AMD.

The future directions of this study are three-fold. First, further work remains to be done to determine the in-depth mechanism of action of phenolic antioxidants in their ability to protect

against oxLDL-induced RPE cell death. As mentioned previously, preliminary data show that hindered phenolic compounds are potentially localized to lysosomal membranes to protect lysosomal integrity from ROS. Elucidating their mechanism would lead to identification of more targeted agents and potentially enable better characterization of the relationship between oxidative stress and inflammation in RPE cells.

Second, compounds related to trolox should be investigated to identify phenolic antioxidants that are more potent in their ability to protect against oxLDL-induced RPE cell death. Our preliminary studies have shown that BHT and PMC, both of which contain a hindered phenol group, displayed higher potency than trolox. The next step would be to use structure-activity relationship analysis to design and synthesize novel analogs of these molecules with higher potency and efficacy in protecting RPE cells.

Finally, the results of these mechanistic studies warrant the testing of phenolic antioxidants in an animal model to evaluate their therapeutic efficacy for dry AMD. While there is no single mouse model that develops all the characteristics of human disease, apoE4-targeted replacement (TR) mice exhibit RPE changes that replicate many of the features of human dry AMD.[75] Thus, aged, high-fat diet-fed apoE4-TR mice will be used as a model to assess whether the phenolic antioxidants prevent the development of AMD-like phenotypes. Ultimately, we hope that these studies will lead to the development of novel therapeutics for dry AMD.

References

1. Evans JR. Risk factors for age-related macular degeneration. *Prog Retin Eye Res*. 2001;20(2):227-253. http://www.ncbi.nlm.nih.gov/pubmed/11173253.

2. Wong WL, Su X, Li X, et al. Global prevalence of age-related macular degeneration and disease burden projection for 2020 and 2040: a systematic review and meta-analysis. *Lancet Glob Heal*. 2014;2(2):e106-16. doi:10.1016/S2214-109X(13)70145-1

3. Jonas JB, Cheung CMG, Panda-Jonas S. Updates on the Epidemiology of Age-Related Macular Degeneration. *Asia-Pacific J Ophthalmol*. 2017;6(6):493-497. doi:10.22608/APO.2017251

4. CATT Research Group, Martin DF, Maguire MG, et al. Ranibizumab and bevacizumab for neovascular age-related macular degeneration. *N Engl J Med*. 2011;364(20):1897-1908. doi:10.1056/NEJMoa1102673

5. Ding X, Patel M, Chan C-C. Molecular pathology of age-related macular degeneration. *Prog Retin Eye Res*. 2009;28(1):1-18. doi:10.1016/j.preteyeres.2008.10.001

6. Suzuki M, Kamei M, Itabe H, et al. Oxidized phospholipids in the macula increase with age and in eyes with age-related macular degeneration. *Mol Vis*. 2007;13:772-778. http://www.ncbi.nlm.nih.gov/pubmed/17563727.

7. Kamei M, Yoneda K, Kume N, et al. Scavenger receptors for oxidized lipoprotein in age-related macular degeneration. *Invest Ophthalmol Vis Sci*. 2007;48(4):1801-1807. doi:10.1167/iovs.06-0699

8. Curcio CA, Johnson M, Huang J-D, Rudolf M. Apolipoprotein B-containing lipoproteins in retinal aging and age-related macular degeneration. *J Lipid Res*. 2010;51(3):451-467. doi:10.1194/jlr.R002238

9. Wang L, Clark ME, Crossman DK, et al. Abundant lipid and protein components of drusen. Koch K-W, ed. *PLoS One*. 2010;5(4):e10329. doi:10.1371/journal.pone.0010329

10. Klein ML. Risk Assessment Model for Development of Advanced Age-Related Macular Degeneration. *Arch Ophthalmol*. 2011;129(12):1543. doi:10.1001/archophthalmol.2011.216

11. Fauser S, Smailhodzic D, Caramoy A, et al. Evaluation of Serum Lipid Concentrations and Genetic Variants at High-Density Lipoprotein Metabolism Loci and *TIMP3* in Age-Related Macular Degeneration. *Investig Opthalmology Vis Sci*. 2011;52(8):5525. doi:10.1167/iovs.10-6827

12. Fritsche LG, Igl W, Bailey JNC, et al. A large genome-wide association study of age-related macular degeneration highlights contributions of rare and common variants. *Nat Genet*. 2016;48(2):134-143. doi:10.1038/ng.3448

13. Mullins RF, Russell SR, Anderson DH, Hageman GS. Drusen associated with aging and age-related macular degeneration contain proteins common to extracellular deposits associated with atherosclerosis, elastosis, amyloidosis, and dense deposit disease. *FASEB J*. 2000;14(7):835-846. http://www.ncbi.nlm.nih.gov/pubmed/10783137.

14. Vingerling JR, Dielemans I, Bots ML, Hofman A, Grobbee DE, de Jong PT. Age-related macular degeneration is associated with atherosclerosis. The Rotterdam Study. *Am J Epidemiol*. 1995;142(4):404-409. http://www.ncbi.nlm.nih.gov/pubmed/7625405.

15. Wilson HL, Schwartz DM, Bhatt HRF, McCulloch CE, Duncan JL. Statin and aspirin therapy are associated with decreased rates of choroidal neovascularization among patients with age-related macular degeneration. *Am J Ophthalmol*. 2004;137(4):615-624. doi:10.1016/j.ajo.2003.10.025

16. Barbosa DTQ, Mendes TS, Cíntron-Colon HR, et al. Age-related macular degeneration and protective effect of HMG Co-A reductase inhibitors (statins): results from the National Health and Nutrition Examination Survey 2005-2008. *Eye (Lond)*. 2014;28(4):472-480. doi:10.1038/eye.2014.8

17. Vavvas DG, Daniels AB, Kapsala ZG, et al. Regression of Some High-risk Features of Age-related Macular Degeneration (AMD) in Patients Receiving Intensive Statin Treatment. *EBioMedicine*. 2016;5:198-203. doi:10.1016/j.ebiom.2016.01.033

18. Beatty S, Koh H, Phil M, Henson D, Boulton M. The role of oxidative stress in the pathogenesis of age-related macular degeneration. *Surv Ophthalmol*. 45(2):115-134. http://www.ncbi.nlm.nih.gov/pubmed/11033038.

19. Datta S, Cano M, Ebrahimi K, Wang L, Handa JT. The impact of oxidative stress and inflammation on RPE degeneration in non-neovascular AMD. *Prog Retin Eye Res*. 2017;60:201-218. doi:10.1016/j.preteyeres.2017.03.002

20. De La Paz M, Anderson RE. Region and age-dependent variation in susceptibility of the human retina to lipid peroxidation. *Invest Ophthalmol Vis Sci*. 1992;33(13):3497-3499. http://www.ncbi.nlm.nih.gov/pubmed/1464495.

21. Rahman I, MacNee W. Role of oxidants/antioxidants in smoking-induced lung diseases. *Free Radic Biol Med*. 1996;21(5):669-681. http://www.ncbi.nlm.nih.gov/pubmed/8891669.

22. Rangasamy T, Cho CY, Thimmulappa RK, et al. Genetic ablation of Nrf2 enhances susceptibility to cigarette smoke–induced emphysema in mice. *J Clin Invest*. 2004;114(9):1248-1259. doi:10.1172/JCI21146

23. Kopitz J, Holz FG, Kaemmerer E, Schutt F. Lipids and lipid peroxidation products in the pathogenesis of age-related macular degeneration. *Biochimie*. 2004;86(11):825-831. doi:10.1016/j.biochi.2004.09.029

24. Hoppe G, O'Neil J, Hoff HF, Sears J. Accumulation of oxidized lipid-protein complexes

alters phagosome maturation in retinal pigment epithelium. *Cell Mol Life Sci*. 2004;61(13):1664-1674. doi:10.1007/s00018-004-4080-5

25. Chou M-Y, Hartvigsen K, Hansen LF, et al. Oxidation-specific epitopes are important targets of innate immunity. *J Intern Med*. 2008;263(5):479-488. doi:10.1111/j.1365-2796.2008.01968.x

26. Berliner JA, Subbanagounder G, Leitinger N, Watson AD, Vora D. Evidence for a role of phospholipid oxidation products in atherogenesis. *Trends Cardiovasc Med*. 11(3-4):142-147. http://www.ncbi.nlm.nih.gov/pubmed/11686004.

27. Schutt F, Bergmann M, Holz FG, Kopitz J. Proteins modified by malondialdehyde, 4-hydroxynonenal, or advanced glycation end products in lipofuscin of human retinal pigment epithelium. *Invest Ophthalmol Vis Sci*. 2003;44(8):3663-3668. http://www.ncbi.nlm.nih.gov/pubmed/12882821.

28. Farboud B, Aotaki-Keen A, Miyata T, Hjelmeland LM, Handa JT. Development of a polyclonal antibody with broad epitope specificity for advanced glycation endproducts and localization of these epitopes in Bruch's membrane of the aging eye. *Mol Vis*. 1999;5:11. http://www.ncbi.nlm.nih.gov/pubmed/10407062.

29. Crabb JW, Miyagi M, Gu X, et al. Drusen proteome analysis: An approach to the etiology of age-related macular degeneration. *Proc Natl Acad Sci*. 2002;99(23):14682-14687. doi:10.1073/pnas.222551899

30. Ambati J, Atkinson JP, Gelfand BD. Immunology of age-related macular degeneration. *Nat Rev Immunol*. 2013;13(6):438-451. doi:10.1038/nri3459

31. Hageman GS, Luthert PJ, Victor Chong NH, Johnson L V, Anderson DH, Mullins RF. An integrated hypothesis that considers drusen as biomarkers of immune-mediated processes at the RPE-Bruch's membrane interface in aging and age-related macular degeneration. *Prog Retin Eye Res*. 2001;20(6):705-732. http://www.ncbi.nlm.nih.gov/pubmed/11587915.

32. Haines JL, Hauser MA, Schmidt S, et al. Complement factor H variant increases the risk of age-related macular degeneration. *Science*. 2005;308(5720):419-421. doi:10.1126/science.1110359

33. Hageman GS, Anderson DH, Johnson L V, et al. A common haplotype in the complement regulatory gene factor H (HF1/CFH) predisposes individuals to age-related macular degeneration. *Proc Natl Acad Sci U S A*. 2005;102(20):7227-7232. doi:10.1073/pnas.0501536102

34. Heurich M, Martínez-Barricarte R, Francis NJ, et al. Common polymorphisms in C3, factor B, and factor H collaborate to determine systemic complement activity and disease risk. *Proc Natl Acad Sci U S A*. 2011;108(21):8761-8766. doi:10.1073/pnas.1019338108

35. Tseng WA, Thein T, Kinnunen K, et al. NLRP3 Inflammasome Activation in Retinal

Pigment Epithelial Cells by Lysosomal Destabilization: Implications for Age-Related Macular Degeneration. *Investig Opthalmology Vis Sci*. 2013;54(1):110. doi:10.1167/iovs.12-10655

36. Tarallo V, Hirano Y, Gelfand BD, et al. DICER1 loss and Alu RNA induce age-related macular degeneration via the NLRP3 inflammasome and MyD88. *Cell*. 2012;149(4):847-859. doi:10.1016/j.cell.2012.03.036

37. Latz E, Xiao TS, Stutz A. Activation and regulation of the inflammasomes. *Nat Rev Immunol*. 2013;13(6):397-411. doi:10.1038/nri3452

38. Sheedy FJ, Grebe A, Rayner KJ, et al. CD36 coordinates NLRP3 inflammasome activation by facilitating intracellular nucleation of soluble ligands into particulate ligands in sterile inflammation. *Nat Immunol*. 2013;14(8):812-820. doi:10.1038/ni.2639

39. Duewell P, Kono H, Rayner KJ, et al. NLRP3 inflammasomes are required for atherogenesis and activated by cholesterol crystals. *Nature*. 2010;464(7293):1357-1361. doi:10.1038/nature08938

40. Menu P, Mayor A, Zhou R, et al. ER stress activates the NLRP3 inflammasome via an UPR-independent pathway. *Cell Death Dis*. 2012;3(1):e261. doi:10.1038/cddis.2011.132

41. Shimada K, Crother TR, Karlin J, et al. Oxidized mitochondrial DNA activates the NLRP3 inflammasome during apoptosis. *Immunity*. 2012;36(3):401-414. doi:10.1016/j.immuni.2012.01.009

42. Gnanaguru G, Choi AR, Amarnani D, D'Amore PA. Oxidized Lipoprotein Uptake Through the CD36 Receptor Activates the NLRP3 Inflammasome in Human Retinal Pigment Epithelial Cells. *Investig Opthalmology Vis Sci*. 2016;57(11):4704. doi:10.1167/iovs.15-18663

43. Age-Related Eye Disease Study Research Group. A Randomized, Placebo-Controlled, Clinical Trial of High-Dose Supplementation With Vitamins C and E, Beta Carotene, and Zinc for Age-Related Macular Degeneration and Vision Loss. *Arch Ophthalmol*. 2001;119(10):1417. doi:10.1001/archopht.119.10.1417

44. Age-Related Eye Disease Study 2 Research Group. Lutein + Zeaxanthin and Omega-3 Fatty Acids for Age-Related Macular Degeneration. *JAMA*. 2013;309(19):2005. doi:10.1001/jama.2013.4997

45. Evans J. Antioxidant supplements to prevent or slow down the progression of AMD: a systematic review and meta-analysis. *Eye*. 2008;22(6):751-760. doi:10.1038/eye.2008.100

46. Lonn E, Bosch J, Yusuf S, et al. Effects of Long-term Vitamin E Supplementation on Cardiovascular Events and Cancer. *JAMA*. 2005;293(11):1338. doi:10.1001/jama.293.11.1338

47. Sheline CT, Zhou Y, Bai S. Light-induced photoreceptor and RPE degeneration involve

zinc toxicity and are attenuated by pyruvate, nicotinamide, or cyclic light. *Mol Vis*. 2010;16:2639-2652. http://www.ncbi.nlm.nih.gov/pubmed/21179242.

48. Yaspan BL, Williams DF, Holz FG, et al. Targeting factor D of the alternative complement pathway reduces geographic atrophy progression secondary to age-related macular degeneration. *Sci Transl Med*. 2017;9(395):eaaf1443. doi:10.1126/scitranslmed.aaf1443

49. Holz FG, Sadda SR, Busbee B, et al. Efficacy and Safety of Lampalizumab for Geographic Atrophy Due to Age-Related Macular Degeneration. *JAMA Ophthalmol*. 2018;136(6):666. doi:10.1001/jamaophthalmol.2018.1544

50. Hong C, Tontonoz P. Coordination of inflammation and metabolism by PPAR and LXR nuclear receptors. *Curr Opin Genet Dev*. 2008;18(5):461-467. doi:10.1016/j.gde.2008.07.016

51. Li AC, Binder CJ, Gutierrez A, et al. Differential inhibition of macrophage foam-cell formation and atherosclerosis in mice by PPARalpha, beta/delta, and gamma. *J Clin Invest*. 2004;114(11):1564-1576. doi:10.1172/JCI18730

52. Lehmann JM, Moore LB, Smith-Oliver TA, Wilkison WO, Willson TM, Kliewer SA. An antidiabetic thiazolidinedione is a high affinity ligand for peroxisome proliferator-activated receptor gamma (PPAR gamma). *J Biol Chem*. 1995;270(22):12953-12956. http://www.ncbi.nlm.nih.gov/pubmed/7768881.

53. Inoue I, Katayama S, Takahashi K, et al. Troglitazone has a scavenging effect on reactive oxygen species. *Biochem Biophys Res Commun*. 1997;235(1):113-116. doi:10.1006/bbrc.1997.6512

54. Kim KY, Ahn JH, Cheon HG. Apoptotic Action of Peroxisome Proliferator-Activated Receptor-γ Activation in Human Non–Small-Cell Lung Cancer Is Mediated via Proline Oxidase-Induced Reactive Oxygen Species Formation. *Mol Pharmacol*. 2007;72(3):674-685. doi:10.1124/MOL.107.035584

55. Wang J, Lv X, Shi J, Hu X, DU Y. Troglitazone induced apoptosis via PPARγ activated POX-induced ROS formation in HT29 cells. *Biomed Environ Sci*. 2011;24(4):391-399. doi:10.3967/0895-3988.2011.04.010

56. Stewart CR, Stuart LM, Wilkinson K, et al. CD36 ligands promote sterile inflammation through assembly of a Toll-like receptor 4 and 6 heterodimer. *Nat Immunol*. 2010;11(2):155-161. doi:10.1038/ni.1836

57. Bauernfeind FG, Horvath G, Stutz A, et al. Cutting edge: NF-kappaB activating pattern recognition and cytokine receptors license NLRP3 inflammasome activation by regulating NLRP3 expression. *J Immunol*. 2009;183(2):787-791. doi:10.4049/jimmunol.0901363

58. Rodrigues GA, Maurier-Mahé F, Shurland D-L, et al. Differential Effects of PPARγ Ligands on Oxidative Stress–Induced Death of Retinal Pigmented Epithelial Cells.

Investig Opthalmology Vis Sci. 2011;52(2):890. doi:10.1167/iovs.10-5715

59. Akinyeke TO, Stewart L V. Troglitazone suppresses c-Myc levels in human prostate cancer cells via a PPARγ-independent mechanism. *Cancer Biol Ther*. 2011;11(12):1046-1058. http://www.ncbi.nlm.nih.gov/pubmed/21525782.

60. Qiao L, Dai Y, Gu Q, et al. Loss of XIAP sensitizes colon cancer cells to PPARγ independent antitumor effects of troglitazone and 15-PGJ2. *Cancer Lett*. 2008;268(2):260-271. doi:10.1016/j.canlet.2008.04.003

61. Coras R, Holsken A, Seufert S, et al. The peroxisome proliferator-activated receptor- agonist troglitazone inhibits transforming growth factor- -mediated glioma cell migration and brain invasion. *Mol Cancer Ther*. 2007;6(6):1745-1754. doi:10.1158/1535-7163.MCT-06-0763

62. Ding Z, Liu S, Wang X, Khaidakov M, Dai Y, Mehta JL. Oxidant stress in mitochondrial DNA damage, autophagy and inflammation in atherosclerosis. *Sci Rep*. 2013;3(1):1077. doi:10.1038/srep01077

63. Joffre C, Leclère L, Buteau B, et al. Oxysterols Induced Inflammation and Oxidation in Primary Porcine Retinal Pigment Epithelial Cells. *Curr Eye Res*. 2007;32(3):271-280. doi:10.1080/02713680601187951

64. Park BC, Thapa D, Lee JS, Park S-Y, Kim J-A. Troglitazone inhibits vascular endothelial growth factor-induced angiogenic signaling via suppression of reactive oxygen species production and extracellular signal-regulated kinase phosphorylation in endothelial cells. *J Pharmacol Sci*. 2009;111(1):1-12. http://www.ncbi.nlm.nih.gov/pubmed/19763043.

65. Gallego-Villar L, Pérez B, Ugarte M, Desviat LR, Richard E. Antioxidants successfully reduce ROS production in propionic acidemia fibroblasts. *Biochem Biophys Res Commun*. 2014;452(3):457-461. doi:10.1016/j.bbrc.2014.08.091

66. Ollinger K, Brunk UT. Cellular injury induced by oxidative stress is mediated through lysosomal damage. *Free Radic Biol Med*. 1995;19(5):565-574. http://www.ncbi.nlm.nih.gov/pubmed/8529915.

67. Arthur PG, Niu X, Rigby P, Steer JH, Jeffrey GP. Oxidative stress causes a decline in lysosomal integrity during hypothermic incubation of rat hepatocytes. *Free Radic Biol Med*. 2008;44(1):24-33. doi:10.1016/j.freeradbiomed.2007.09.003

68. DeForge LE, Preston AM, Takeuchi E, Kenney J, Boxer LA, Remick DG. Regulation of interleukin 8 gene expression by oxidant stress. *J Biol Chem*. 1993;268(34):25568-25576. http://www.ncbi.nlm.nih.gov/pubmed/8244994.

69. Chandel NS, Trzyna WC, McClintock DS, Schumacker PT. Role of oxidants in NF-kappa B activation and TNF-alpha gene transcription induced by hypoxia and endotoxin. *J Immunol*. 2000;165(2):1013-1021. http://www.ncbi.nlm.nih.gov/pubmed/10878378.

70. Song C, Mitter SK, Qi X, et al. Oxidative stress-mediated NFκB phosphorylation upregulates p62/SQSTM1 and promotes retinal pigmented epithelial cell survival through increased autophagy. Srinivasula SM, ed. *PLoS One*. 2017;12(2):e0171940. doi:10.1371/journal.pone.0171940

71. Zhang J, Zhang Y, Xiao F, et al. The peroxisome proliferator-activated receptor γ agonist pioglitazone prevents NF-κB activation in cisplatin nephrotoxicity through the reduction of p65 acetylation via the AMPK-SIRT1/p300 pathway. *Biochem Pharmacol*. 2016;101:100-111. doi:10.1016/j.bcp.2015.11.027

72. Liu T, Zhang L, Joo D, Sun S-C. NF-κB signaling in inflammation. *Signal Transduct Target Ther*. 2017;2:17023. doi:10.1038/sigtrans.2017.23

73. Tafazoli S, Wright JS, O'Brien PJ. Prooxidant and antioxidant activity of vitamin E analogues and troglitazone. *Chem Res Toxicol*. 2005;18(10):1567-1574. doi:10.1021/tx0500575

74. Ablonczy Z, Dahrouj M, Tang PH, et al. Human retinal pigment epithelium cells as functional models for the RPE in vivo. *Invest Ophthalmol Vis Sci*. 2011;52(12):8614-8620. doi:10.1167/iovs.11-8021

75. Malek G, Johnson L V, Mace BE, et al. Apolipoprotein E allele-dependent pathogenesis: a model for age-related retinal degeneration. *Proc Natl Acad Sci U S A*. 2005;102(33):11900-11905. doi:10.1073/pnas.0503015102

Acknowledgements

First, I am deeply grateful to my mentor, Dr. Patricia D'Amore, for her extraordinary mentorship. She has encouraged me to grow as a scientist by constantly challenging me to think critically. I feel incredibly fortunate to have had the opportunity to carry out this meaningful work under her guidance. Furthermore, she has always been generous in offering me advice about life and career. She continues to inspire me through her dedication to mentorship, enthusiasm for science, and warmth as a person.

I am equally indebted to my colleagues in the D'Amore lab. I would like to express my sincere gratitude to Dr. Gopalan Gnanaguru for his day-to-day mentorship and assistance with carrying out various experiments. Our discussions about study design, techniques, and data analysis form the basis of much of this work. I am also thankful to Dr. Eric Ng for his valuable input regarding the project, often through late-night conversations in the lab, and for his help with putting this thesis together. Special thanks to Dhanesh Amarneni and Ashley Mackey for teaching me various techniques, to Dian Li for his assistance with ImageJ analysis, and to all of my fellow labmates for making research a fun and enjoyable endeavor.

Additionally, I would like to extend my gratitude to the Harvard-M.I.T. Health Sciences and Technology (HST) program for supporting my research, and to Dr. Rick Mitchell, Patty Cunningham, and Karrol Rikka Altajeros for their thoughtful advice and unwavering support throughout my time at HST.

Finally, I would like to thank my family and friends for their unconditional love and encouragement. They are the ones who have kept me strong and resilient; without them, this work would not have been possible.